NUMERICAL SIMULATION OF INJECTION MOULD-FILLING AND OPTIMIZATION OF MOULDING CONDITIONS FOR A CYLINDRICAL OBJECT

By

AMIT KUMAR

DEPARTMENT OF MECHANICAL ENGINEERING

INDIAN INSTITUTE OF TECHNOLOGY, KANPUR

JULY, 1998

ME
1998
M
[redacted] AMI
NUM

NUMERICAL SIMULATION OF INJECTION MOULD-FILLING AND OPTIMIZATION OF MOULDING CONDITIONS FOR A CYLINDRICAL OBJECT

A Thesis Submitted

in Partial Fulfilment of the Requirements

for the Degree of

Master of Technology

by

AMIT KUMAR

to the

DEPARTMENT OF MECHANICAL ENGINEERING

INDIAN INSTITUTE OF TECHNOLOGY KANPUR

July 1998

POST GRADUATE OFFICE
I.I.T. Kanpur
Submitted on 13.7.98

CERTIFICATE

It is certified that the work contained in the thesis entitled **Numerical Simulation of injection Mould-Filling and Optimization of Moulding Conditions for a Cylindrical Object**, by **Amit Kumar** , has been carried out under our supervision and that this work has not been submitted elsewhere for a degree.

Dr P S. Ghoshdastidar
Associate Professor
Department of Mechanical Engineering
I.I T. Kanpur

Prof. M.K.Muju
Professor
Department of Mechanical Engineering
I.I.T. Kanpur

July 1998

Abstract

In the present work, numerical simulation of the mould-filling for the production of a cylindrical object using low density polyethylene(LDPE) as the material is presented first. The final part of this thesis deals with optimization of moulding condition and material selection. Finite-difference method is used for the purpose of modelling. Three cases have been considered, namely (*i*) Isothermal filling at constant injection pressure, (*ii*) Isothermal filling at constant flow rate and (*iii*) Non-isothermal filling at constant flow rate. The results show excellent tally with the corresponding analytical solutions for the first two cases showing the correctness of the numerical method. The simulation results for non-isothermal filling show physically realistic trends and lend insight into various important aspect of mould-filling including frozen skin layer. The optimization study which uses exhaustive search method is based on the simulation results for non-isothermal filling and also considers cooling of the object. The data for cooling have been taken from a published experimental work. It is found that between LDPE and Polypropylene, the latter is a better material for the production of this object.

Acknowledgement

I would like this opportunity to express my sincere gratitude to my thesis supervisors Dr. M. K. Muju and Dr. P. S. Ghoshdastidar for their sincere help, fruitful suggestions and inspiration during my entire course of this work. I am extremely thankful to them for giving me complete freedom of work, thus helping me to gain confidence and to work independently.

Special thanks and gratitude are due to Professor G.K.Lal who allowed me to use C-MOLD 3DQUICKFILL software of the A C Technology Inc, USA. Although the software was not directly used in this thesis, it gave me good insight into the injection moulding process.

I am also very much thankful to my friends Jyoti, Vipin and others for their allround support, encouragement and suggestions.

I wish to express my indebtedness to my parents and sisters whose deep affection and silent inspiration have always guided me towards success.

Amit Kumar

Contents

Abstract i

Acknowledgement ii

Contents iii

List of Figures vi

List of Tables viii

Nomenclature x

1 INTRODUCTION 1

1.1 Literature Review 4

1.2 Objectives of the present work 5

1.3 Organization of thesis 5

2 PROBLEM FORMULATION AND METHOD OF SOLUTION 7

2.1 Isothermal Filling of Cavity at Constant Injection Pressure . 8

2.1.1 Problem Statement 8

2.1.2 Formulation 8

2.1.3 Details of Finite Difference Formulation 10

2.1.4 Method of Solution 12

2 2 Isothermal Filling of Cavity at Constant Flow rate 13

2.2.1 Problem Statement 13

2.2.2 Formulation 13

2.2.3 Details of Finite Difference Formulation 16

2.2.4 Method of Solution 18

2 3 Non-Isothermal Filling of Cavity at Constant Flow Rate 20

2.3.1 Problem Statement 20

2.3.2 Formulation 20

2.3.3 Details of Finite Difference Formulation 22

2.3.4 Average Melt Temperature 26

2.3.5 Stability Criterion 26

2.3.6 Method of Solution 26

3 RESULTS AND DISCUSSION 29

3.1 CASE I : Isothermal Filling : Constant Injection Pressure 30

3.2 CASE II: Isothermal Filling : Constant Flow Rate 32

3.3 CASE III: Non-Isothermal Filling : Constant Flow Rate 34

4 OPTIMIZATION OF MOULDING CONDITIONS AND MATERIAL SELECTION 41

4.1 Characteristics of Process 42

4.2 Quality Measures 42

4.2.1 Temperature Difference 44

4.2.2 Pressure 45

4.3 The Basic Method of Optimization 45

4.3.1 Determination of Approximate Feasible Moulding Space (AFMS) 46

4.3 2 Material Selection Based on AFMS 46
4.3.3 Optimization of Moulding Conditions 47
4.4 Results 47

5 CONCLUSIONS AND SCOPE FOR FUTURE WORK 59
5 1 Scope For Future Work 60

Bibliography 61

Appendix A 62

Appendix B 64

List of Figures

1.1 Figure of Injection Moulding Machine. 3

2.1 Cylinderical cavity to be filled by polymer melt 8

2.2 Computational domain for isothermal filling of cylindrical cavity at constant injection pressuree. 9

2.3 Grid for isothermal filling of cylindrical cavity at constant injection pressure 11

2.4 Flow chart of algorithm to simulate the isothermal filling of cylindrical cavity at constant injection pressure. 14

2.5 Computational domain for isothermal filling of cylindrical cavity at constant flow rate. 15

2.6 Grid for isothermal filling of cylindrical cavity at constant flow rate 17

2.7 Flow chart of algorithm to simulate the isothermal filling of cylindrical cavity at constant flow rate. 19

2.8 Computational domain for non-isothermal filling of cylindrical cavity. 21

2.9 Grid for non-isothermal filling of cylindrical cavity. 24

2.10 FLow chart of algorithm to simulate the non-isothermal filling of cylindrical cavity. 28

3.1 Position of advancing melt front as a function of time for constant injection pressure isothermal filling. 31

3.2 Flow rate versus axial distance for constant injection pressure isothermal filling. 32

3.3 Melt velocity profile at various Z-locations for constant injection pressure isothermal filling. 32

3.4 Plot of injection pressure versus time for constant flow rate isothermal filling. 34

3.5 Comparison of injection pressure versus time for non-isothermal and isothermal filling at constant flow rate. 35

3.6 Melt temperature fields at various z-locations for $Q = 0.515X10^{-4}$ (m^3/s). 37

3.7 Melt temperature fields at various z-locations for $Q = 0\ 107X10^{-4}$ (m^3/s). 37

3.8 "Frozen skin" layer for various flow rates. 38

3.9 "Pressure distribution in the cavity after filling. 39

3.10 Shape and location of the melt front at various times. 40

List of Tables

3.1 Input Data for Case I(Tadmor and Gogos,1979) 30

3.2 Values of t and Q at various Z 31

3.3 Input Data for Case II(Tadmor and Gogos,1979) 33

3.4 Comparison of $P_{inj,anal}$ and $P_{inj,numl.}$ Vs t 33

3.5 Input Data for Case III 35

4.1 Mould temperature=60°C, Melt temeperature=200°C for LDPE . 49

4.2 Mould temperature=60°C, Melt temeperature=240°C for LDPE . 50

4.3 Mould temperature=80°C, Melt temeperature=200°C for LDPE . 51

4.4 Mould temperature=80°C, Melt temeperature=240°C for LDPE . 52

4.5 Approximate Feasible Moulding Space for LDPE 52

4.6 Comparisons of Result at Serial No. 1 of AFMS shown in Table 4.5 and result after optimization for LDPE 53

4.7 Comparisons of Result at Serial No.2 of AFMS shown in Table 4.5 and result after optimization for LDPE 54

4.8 Comparisons of Result at Serial No.3 of AFMS shown in Table 4.5 and result after optimization for LDPE 54

4.9 Comparisons of Result at Serial No.4 of AFMS shown in Table 4.5 and result after optimization for LDPE 55

4.10 Comparisons of Result at Serial No.5 of AFMS shown in Table 4.5 and result after optimization for LDPE 55

4.11 Comparisons of Result at Serial No.6 of AFMS shown in Table 4.5 and result after optimization for LDPE 56

4.12 Comparisons of Result at Serial No.7 of AFMS shown in Table 4.5 and result after optimization for LDPE 56

4.13 Comparisons of Result at Serial No.8 of AFMS shown in Table 4.5 and result after optimization for LDPE 57

4.14 Approximate Feasible Moulding Space for POLYPROPYLENE 58

5.1 Input Data for LDPE(Bown,1979) 65

5.2 Input Data for Polypropylene(Bown,1979) 65

Nomenclature

b	Temperature coefficient of viscosity ($^{\circ}C^{-1}$)
C_p	Specific heat at constant pressure ($J/kg^{\circ}C$)
D	Diameter (m)
h	Melt-mould thermal contact resistance coefficient ($W/m^2\ ^{\circ}C$)
k	Thermal conductivity ($W/m^{\circ}C$)
L	Length(m)
m	Consistency index (Ns^n/m^2)
n	Power law index
P	Pressure (Pa)
P_{inj}	Injection Pressure (Pa)
P_{mc}	Maximum allowable injection pressure (Pa)
Q	Flow rate (m^3/s)
R	Radius (m)
T	Temperature ($^{\circ}C$)
T_{avg}	Averaege temperature of the melt ($^{\circ}C$)

T_i	Inlet melt temperature ($°C$)
T_{melt}	Inlet melt temperature ($°C$)
T_{mould}	Mould temperature ($°C$)
T_x	Heat distortion temperature ($°C$)
t	Filling time (sec)
t_c	Cooling time (sec)
V_z	Velocity in the z-direction (m/s)
V_{zavg}	Average velocity of the melt (m/s) ($= \frac{\int_0^R V_z 2\pi r dr}{\pi R^2}$)
r	Radial coordinate (m)
z	Axial coordinate (m)

Greek letters

T_α	Ejection temperature of moulding(heat distortion temperature) ($°C$)
α	Thermal diffusivity (m^2/s)
ϵ	A very small value
μ	Viscosity (Ns/m^2)
μ_0	Viscosity at zero shear (Ns/m^2)
ρ	Density of the material (kg/m^3)
τ_{rz}	Shear stress (N/m^2)

Subscripts

i	inlet, grid index in z-direction
inj	injection
j	grid index in r-direction
$melt$	For melt
$mould$	For mould
max	Maximum
min	Minimum
c	Cooling

Special symbol

Δ	increment

Chapter 1

INTRODUCTION

Injection moulding is one of the most important polymeric processes for producing thermoplastic products. Wherever one cares to look around in the home, the office, the factory, in industry, agriculture, horticulture or , in all aspects of modern life, one sees injection moulded plastic products. Approximately 32% of all plastic products are produced by injection moulding (Pandelidis and Zou.,1990). This process is a complex but highly efficient means of producing a large variety of thermoplastic products, particularly those with high production requirements, tight tolerances and complex shapes.

Injection moulding is a process in which a plastic moulding material is fed in solid form, to a machine where it is heated to be softened or plasticized and is then forced under pressure into a mould. In the mould it cools and hardens and in its hardened state can be ejected from the mould which can then be closed and the cycle of operation is repeated.

The injection moulding machine shown in Fig 1.1 consists of three basic components:

1. A power unit, generally a hydraulic pressure system in which an electric motor is used to drive a hydraulic pump to produce hydraulic pressure in a fluid which can then be piped to the the various sections of the

machine to actuate the moving parts

2. A plasticizing unit for heating and softening the plastic and for forcing the softened material into a mould. This is generally achieved by a plunger, close-fitting to the bore of the cylinder, which is moved forwards and backwards by hydraulic power.
3. A split mould which can be held closed against the pressure of the injected material and opened to remove the resultant moulding.

The injection moulding is a cyclic process. During the filling stage , the injection pressure in the mould rises slowly. as the molten, non-Newtonian. polymer spreads to fill the empty cold cavity. The flow is unsteady, and the polymer starts to cool as soon as it touches the cold walls of the mould. Melt flow does not cease when it reaches the end of cavity. It is then desirable to introduce more polymer into the cavity during the packing stage, in order to compensate for shrinkage due to continuous cooling. The viscous polymer is, therefore, compressed , and the cavity pressure rises to a peak. Cooling, however, through heat exchange with the cavity wall, causes the melt to solidify. Thus in the solidification stage, a continuous decrease in the cavity pressure is observed.

To improve the mould design and process control in this area, increasing reliance has been placed on computer-aided design, manufacture and engineering. The quality of an injection moulded part is affected by many factors which include geometric parameters associated with the mould design and the cooling system design as well as process parameters such as the moulding conditions during the filling phase . This thesis presents an approach to simulate the filling of injection moulding process and to optimize the moulding conditions. The analysis of filling stage is based on finite difference numerical solution which can handle cylindrical parts with aspect ratio up to 100:1. The optimization problem is broken here into three parts. An approximate feasible moulding space is first determined to construct the search space for the optimization algorithm. Quality is quantified as a function of flow simulation

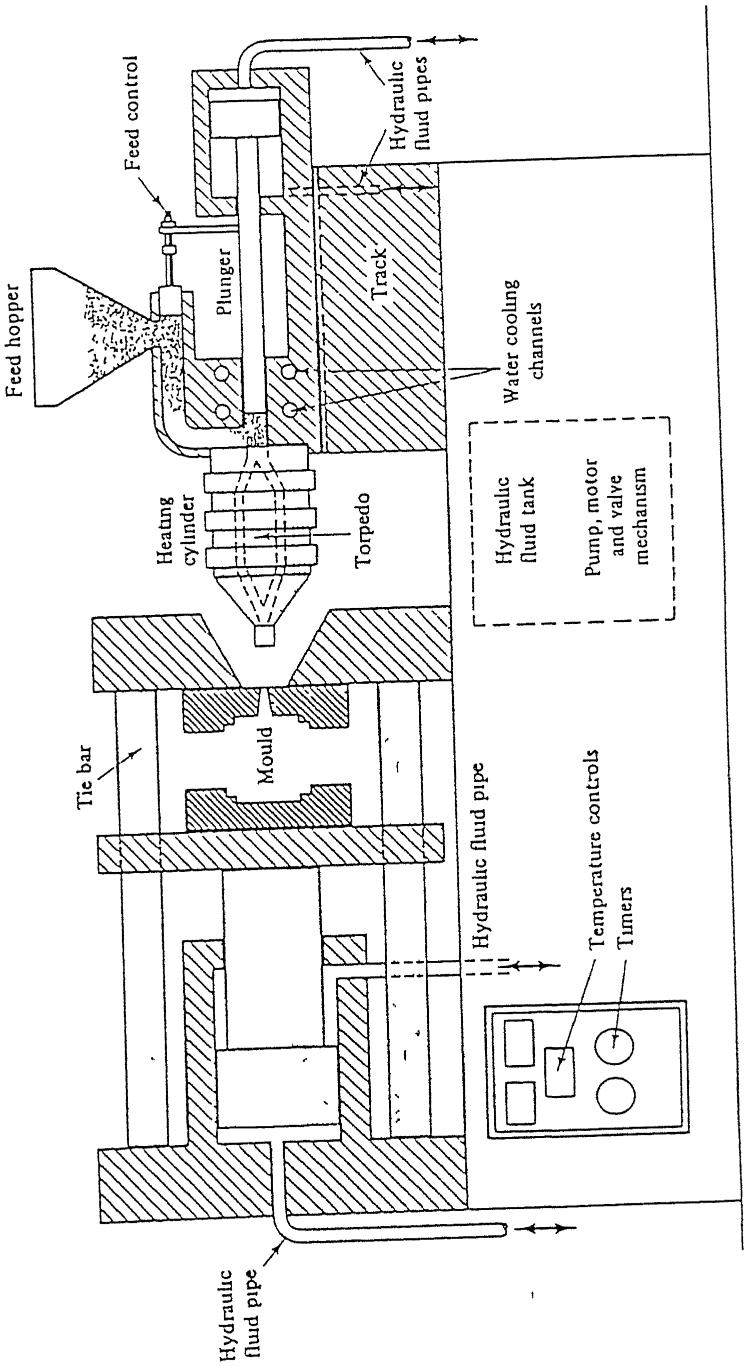

Figure 1.1: Figure of Injection Moulding Machine.

outputs and constitutes the objective function that must be minimized. The resulting optimization is solved by an exhaustive search in the constrained space.

1.1 Literature Review

Lots of work have been done on numerical simulation of cavity-filling process but very less attention has been given to optimization of the moulding conditions However, in recent years attempts have been made to optimize the processing parameters

Numerous mathematical models have been proposed and extensively developed by various research groups for the analysis of different stages of injection moulding process. Serious research on injection moulding started with work of Spencer and Gillmore (1952)(Kamal et al. 1989), in early fifties. They used an empirical equation for capillary flow, coupled with a quasi steady approximation and developed a correlation to calculate the filling time associated with the moulding process. A numerical model for disk type geometry was given by Kamal and Kenig (1972) who proposed an integrated mathematical treatment of the filling, packing and cooling stages of the injection moulding cycle. For the analysis of the filling stages, equation of continuity, motion and energy were simplified under certain assumptions. Wu et al. (1974), also presented a model for simulation of the mould filling process of a disk shaped cavity The transport equations for a power law fluid are used to solve the transient and non-isothermal problem of filling a disk -shaped cavity. A finite difference/finite element simulation was presented by Hieber and Shen (1980). In this model a detailed formulation was presented for simulating the injection mould filling of thin cavities of arbitrary planer geometry. The modelling is in terms of generalised Hele-Shaw flow for an inelastic, non-Newtonian fluid under non-isothermal conditions. For simulation of post filling stages Chiang et al. (1991) presented a unified simulation of the filling and post filling stages in injection moulding. They employed a unified theoretical model to simulate the filling and post filling stages of the injection moulding process. Implementation of such a model is based on hybrid finite element/finite difference numerical solution of the generalized Hele-Shaw flow of a compressible viscous fluid under non-isothermal conditions. Hetu et al. (1998) has reported a 3D finite element method for the simulation of the filling stage in injection moulding.

Some works have been done to select the optimum moulding condition In this direction Pandelidis and Zou (1990) have done some research. In their study, the problem of automatic optimization of gate location is addressed and a methodology for moulding condition optimization is presented. Now some researchers have started using advanced technique like Neural Networks for optimizing moulding conditions. Choi et al. (1994) presented a method to optimize process parameters of injection moulding with Neural Network application in a process simulation environment. In their study a learning system has been developed to generate an optimum set of process parameters at the design stage with minimum number of CAE simulation runs.

1.2 Objectives of the present work

1. To simulate the filling stage in injection moulding of a cylindrical object.
2. Optimization of the moulding conditions on the basis of simulation results.

1.3 Organization of thesis

Chapter 2 deals with problem statement, method of solution, their respective governing equations and boundary conditions for isothermal and non-isothermal filling of cylindrical cavity. For isothermal filling, the cases of constant flow rate (the usual production method) and constant injection pressure has been discussed. But for the non-isothermal case, only constant flow rate problem has been discussed. This chapter also deals with the details of finite difference formulations and the solution procedures.

Chapter 3 contains the results and discussion

Chapter 4 describes a method of optimization of moulding conditions and material selection. It also reports the results based on optimization.

Chapter 5 comprises the conclusions and suggestions for the future work.

Chapter 2

PROBLEM FORMULATION AND METHOD OF SOLUTION

The analysis of injection mould filling represents a major application of computer modelling in polymer processing. The problem is challenging because of the moving melt front, the non-Newtonian nature of the flow and temperature dependent viscosity of the polymer melt.

In this chapter, the simulation of isothermal and non-isothermal filling of a cylindrical cavity which is fed isothermally through a tubular "runner" is discussed. The geometry of the cavity to be filled is shown in Fig.2.1.

We consider the transient filling of such a cavity with non-Newtonian melt under isothermal and non-isothermal conditions. There are two possible cases:

1. Constant flow rate(the usual production method)
2. Constant injection pressure.

In either case we assume that the runner has a small volume by comparison to that of the cavity itself. This allows the assumption that the runner is always filled and that the transient is associated only with filling of the cavity.

2.1 Isothermal Filling of Cavity at Constant Injection Pressure

2.1.1 Problem Statement

Consider the quasi-steady, fully developed, incompressible flow of a polymer melt along a circular tube of diameter D and length L (shown in Fig 2.1) under isothermal conditions. The polymer is assumed to follow power law viscosity model. The melt is injected in mould at constant pressure P_{inj} and temperature T_i. Here, due to constant injection pressure throughout filling, flow rate Q decreases as mould fills

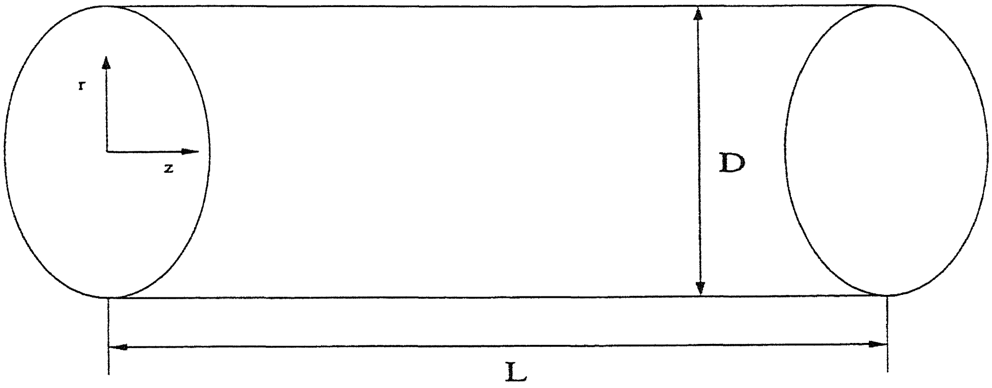

Figure 2.1: Cylindrical cavity to be filled by polymer melt

2.1.2 Formulation

Cylindrical polar co-ordinates r and z are appropriate for describing the axi-symeteric flow, in which the there is no variations with respect to the third angular co-ordinate, θ and $V_\theta = 0$. Fully developed flow implies that $\frac{\partial V_z}{\partial Z} = 0$. From the equation of continuity it can be deduced that $V_r = 0$.

Since, the problem is thermally and geometrically symmetric about the longitudinal axis, only one half of the physical domain is considered. The computational domain is shown in Fig.2.2.

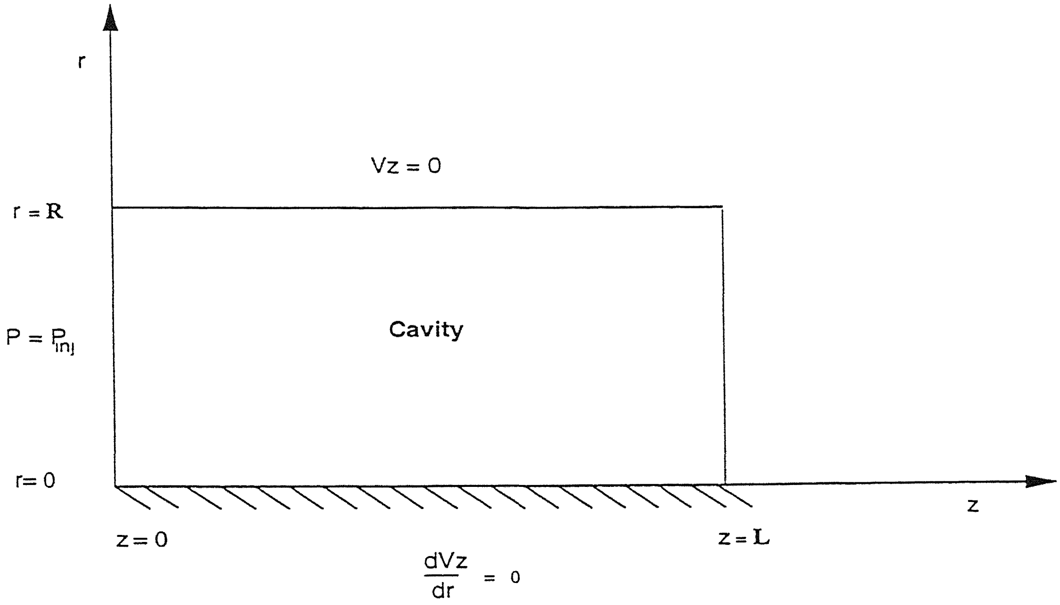

Figure 2.2: Computational domain for isothermal filling of cylindrical cavity at constant injection pressuree.

Governing Differential Equation:

Turning to the equation of motion, the three components of the equation reduces to,

$$\frac{\partial P}{\partial r} = 0 \tag{2.1}$$

$$\frac{\partial P}{\partial \theta} = 0 \tag{2.2}$$

$$\frac{\partial P}{\partial Z} = \frac{1}{r}\frac{\partial}{\partial r}\left(r\tau_{rz}\right) \tag{2.3}$$

where,

$$\tau_{rz} = \mu\,\frac{\partial V_z}{\partial r}$$

and,

$$\mu = m|\frac{\partial V_z}{\partial r}|^{n-1}.$$

for Power law fluid.

Clearly P is a function of only Z, whereas right-hand side of Eq.(2.3) is a function of only r. Eq.(2.3) is the governing differential equation for this case.

Boundary Conditions:

$$B\,C\,1 \quad r=0, \frac{\partial V_z}{\partial r}=0 \quad (axi-symmetry)$$

$$B.C.2 \quad r=R, V_z=0 \qquad (no-slip)$$

The pressure at the melt front is always zero because the atmospheric pressure prevails there, so $P_{meltfront}=0$(Guceri,1989).

2.1.3 Details of Finite Difference Formulation

Simplifying Eq.(2.3), we get

For $r=0$

$$\frac{\partial P}{\partial Z}=2\mu\frac{\partial V_z}{\partial r} \tag{2.4}$$

and,

$$\mu=\mu_0$$

where μ_0 is viscosity at zero shear .

For $r>0$

$$\frac{\mu}{r}\frac{\partial V_z}{\partial r}+\mu\frac{\partial^2 V_z}{\partial r^2}+\frac{\partial\mu}{\partial r}\frac{\partial V_z}{\partial r}-\frac{\partial P}{\partial Z}=0 \tag{2.5}$$

and,

$$\mu=m\left|\frac{\partial V_z}{\partial r}\right|^{n-1},$$

for Power law fluid.

The grid is shown in Fig.2.3.

Depending upon the locations of grid points two-point/three-point forward/backward/central difference schemes of first/second order of accuracy for various derivatives appearing in Eq.(2.4) and Eq.(2.5) have been used. A grid of any size can be used.

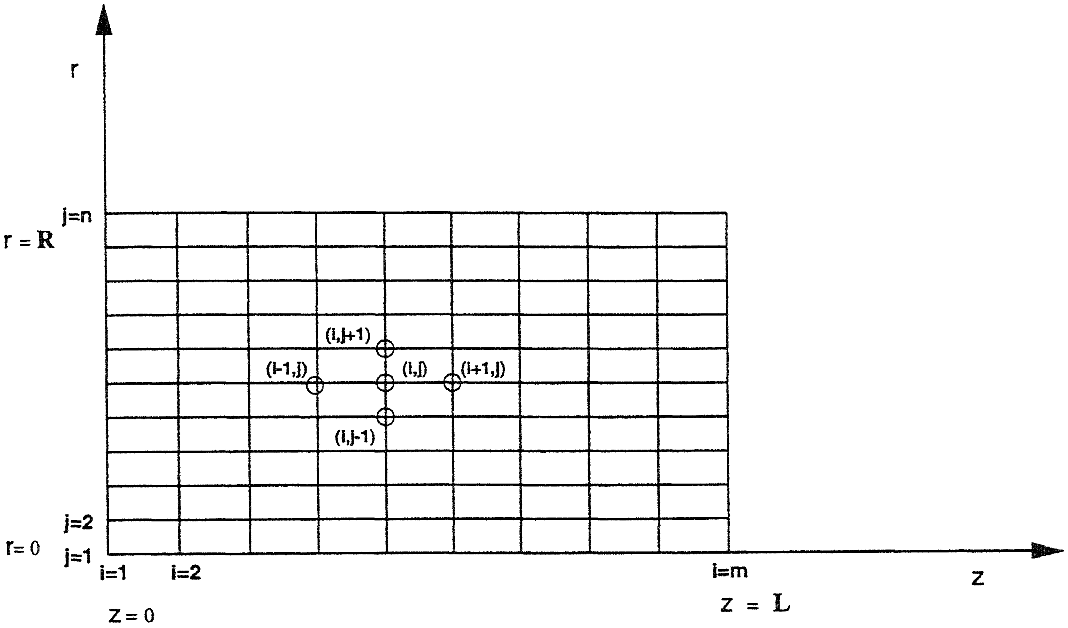

Figure 2.3: Grid for isothermal filling of cylindrical cavity at constant injection pressure.

Grid Point : i=1, j=1

This grid point corresponds to $r = 0$ and hence Eq.(2.4) applies here.

Since, $\frac{\partial V_z}{\partial r} = 0$, using image point technique, we have,

$$\frac{V_{z\,i,j+1} - V_{z\,i,j-1}}{2\Delta r} = 0$$

$$\Rightarrow V_{z\,i,j+1} = V_{z\,i,j-1}$$

Since, $P_{meltfront} = 0$, i.e $P_{i+1,j} = 0$

Hence, the finite difference approximation of G.D.E becomes

$$4\frac{\mu_{i,j}}{\Delta r^2}V_{z\,i,j} - 4\frac{\mu_{i,j}}{\Delta r^2}V_{z\,i,j+1} - \frac{P_{i,j}}{Z} = 0 \tag{2.6}$$

Grid Point : i=2, j=2,n-2

The finite difference approximation of the Eq.(2.5) is,

$$V_{z\,i,j-1}\left(-\frac{\mu_{i,j}}{2\Delta r\; r_{i,j}} + \frac{\mu_{i,j}}{\Delta r^2} - \frac{\mu_{i,j+1} - \mu_{i,j-1}}{4\Delta r^2}\right) + V_{z\,i,j}\left(-2\frac{\mu_{i,j}}{\Delta r^2}\right)$$

$$+V_{z\,i,j+1}\left(\frac{\mu_{i,j}}{2\Delta r\; r_{i,j}} + \frac{\mu_{i,j}}{\Delta r^2} + \frac{\mu_{i,j+1} - \mu_{i,j-1}}{4\Delta r^2}\right) + \frac{P_{i,j}}{Z} = 0 \tag{2.7}$$

Grid Point : i=2, j=n-1

The finite difference approximation of the Eq.(2.5) is,

$$V_{z\,i,j-1}\left(-\frac{\mu_{i,j}}{2\Delta r\; r_{i,j}} + \frac{\mu_{i,j}}{\Delta r^2} - \frac{\mu_{i,j+1} - \mu_{i,j-1}}{4\Delta r^2}\right)$$

$$+V_{z\,i,j}\left(-2\frac{\mu_{i,j}}{\Delta r^2}\right) + \frac{P_{i,j}}{Z} = 0 \tag{2.8}$$

2.1.4 Method of Solution

A direct solution method or implicit method has been used to solve the governing differential equation. Once the set of linear simultaneous equations is obtained, the problem is to solve these equations.To solve the set of linear simultaneous algebraic equations arising out of the discretization of the governing differential equation, the Thomas algorithm has been used. The solution gives us velocity profile of melt in the cavity. This velocity profile has been used to find time of filling and pressure distribution in the cavity. The

The accuracy of the solution depends on the grid spacing in r and z-direction. The whole algorithm for simulation of the process is shown in the flow chart, Fig 2.4 To calculate the filling time, an integrated average velocity (V_{zavg}) which is evaluated from the velocity profile is used. The expression for V_{zavg} is given in the Nomenclature.

2.2 Isothermal Filling of Cavity at Constant Flow rate

2.2.1 Problem Statement

Consider the quasi-steady, fully-developed, incompressible flow of a polymer melt along a circular tube of diameter D and length L (shown in Fig.2.1) under isothermal conditions. The melt is injected at temperature T_i into the cavity, to attain constant flow rate Q the injection pressure P_{inj} is increased as the cavity fills.

2.2.2 Formulation

Cylindrical polar co-ordinates r and z are appropriate for describing the axi-symeteric flow, in which the there is no variations with respect to the third angular co-ordinate, θ and $V_\theta = 0$. Fully developed flow implies that $\frac{\partial V_z}{\partial Z} = 0$. From the equation of continuity it can be deduced that $V_r = 0$.

Since, the problem is thermally and geometrically symmetric about the longitudinal axis, only one half of the physical domain is considered. The computational domain is shown in Fig.2.5.

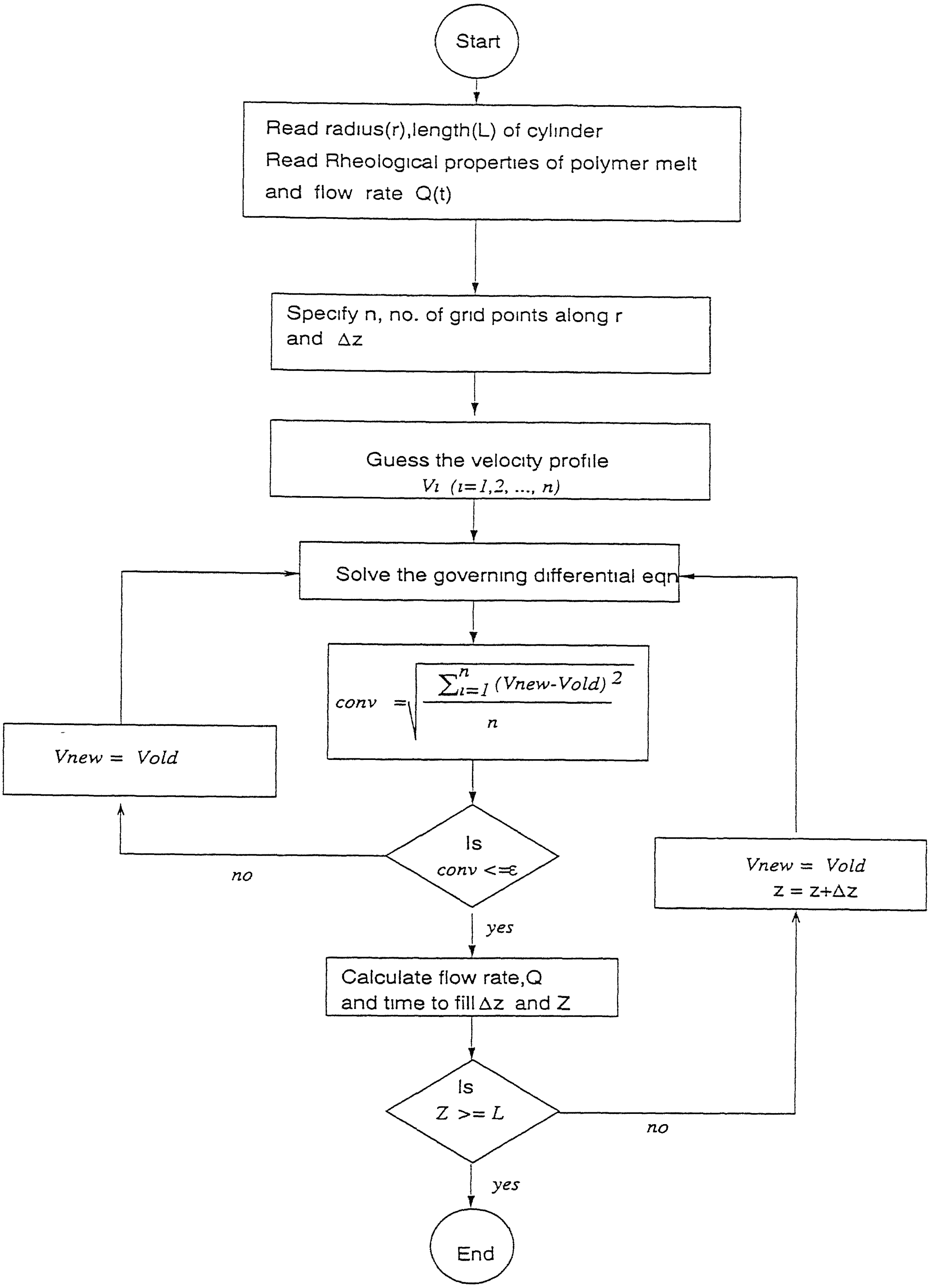
Start
Read radius(r),length(L) of cylinder
Read Rheological properties of polymer melt
and flow rate Q(t)
Specify n, no. of grid points along r
and Δz
Guess the velocity profile
$V_i\ (i=1,2,...,n)$
Solve the governing differential eqn
$conv = \sqrt{\frac{\sum_{i=1}^{n}(Vnew-Vold)^2}{n}}$
Vnew = Vold
Is
conv <=ε
no
yes
Vnew = Vold
z = z+Δz
Calculate flow rate,Q
and time to fill Δz and Z
Is
Z >= L
no
yes
End

Figure 2.4: Flow chart of algorithm to simulate the isothermal filling of cylindrical cavity at constant injection pressure.

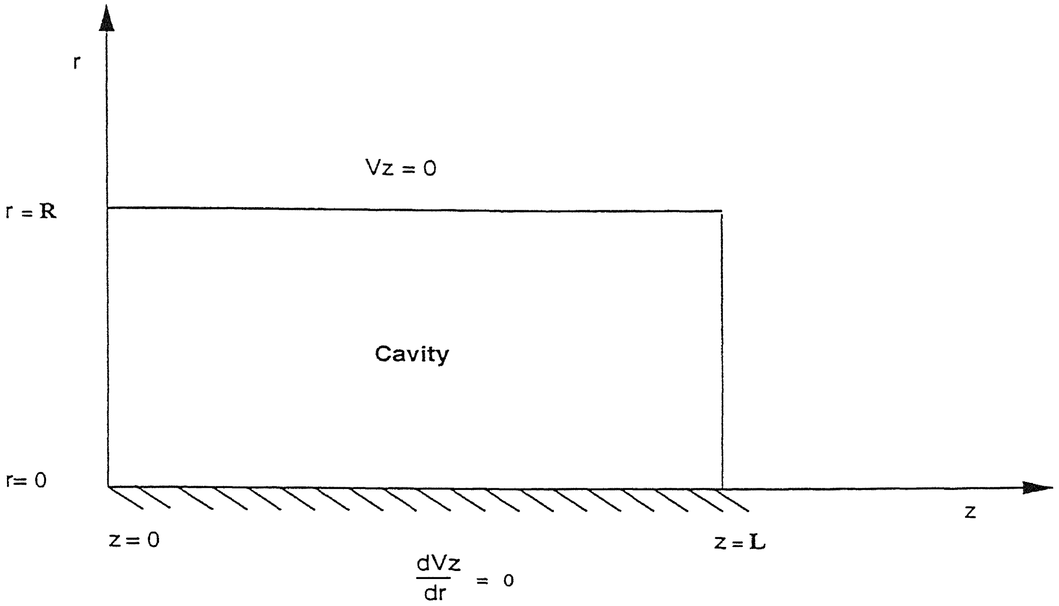

Figure 2.5: Computational domain for isothermal filling of cylindrical cavity at constant flow rate.

Governing Differential Equation:

Turning to the equation of motion. the three components of the equation reduces to,

$$\frac{\partial P}{\partial r} = 0 \tag{2.9}$$

$$\frac{\partial P}{\partial \theta} = 0 \tag{2.10}$$

$$\frac{\partial P}{\partial Z} = \frac{1}{r}\frac{\partial}{\partial r}(r\tau_{rz}) \tag{2.11}$$

where,

$$\tau_{rz} = \mu \frac{\partial V_z}{\partial r}$$

and,

$$\mu = m\left|\frac{\partial V_z}{\partial r}\right|^{n-1},$$

for Power law fluid.

Clearly P is a function of only Z, whereas right-hand side of Eq.(2 11) is a function of only r. Eq.(2.11) is the governing differential equation for this case.

Boundary Conditions:

$$
\begin{aligned}
&B\,C\,1 \quad r = 0, \frac{\partial V_z}{\partial r} = 0 \quad (axi - symmetry)\\
&B.C.2 \quad r = R, V_z = 0 \qquad\qquad (no - slip)
\end{aligned}
$$

The pressure at the melt front is always zero because the atmospheric pressure prevails there, so $P_{meltfront} = 0$ [illegible]

2.2.3 Details of Finite Difference Formulation

Simplifying Eq.(2.11), we get

For $r = 0$

$$\frac{\partial P}{\partial Z} = 2\mu \frac{\partial V_z}{\partial r} \tag{2.12}$$

and,

$$\mu = \mu_0$$

where μ_0 is viscosity at zero shear .

For $r > 0$

$$\frac{\mu}{r}\frac{\partial V_z}{\partial r} + \mu \frac{\partial^2 V_z}{\partial r^2} + \frac{\partial \mu}{\partial r}\frac{\partial V_z}{\partial r} - \frac{\partial P}{\partial Z} = 0 \tag{2.13}$$

and,

$$\mu = m\left|\frac{\partial V_z}{\partial r}\right|^{n-1}$$

The grid is shown in Fig.2.6.

Depending upon the locations of grid points two-point/three-point forward/backward/central difference schemes of first/second order of accuracy for various derivatives appearing in Eq.(2.12) and Eq.(2.13) have been used. A grid of any size can be used.

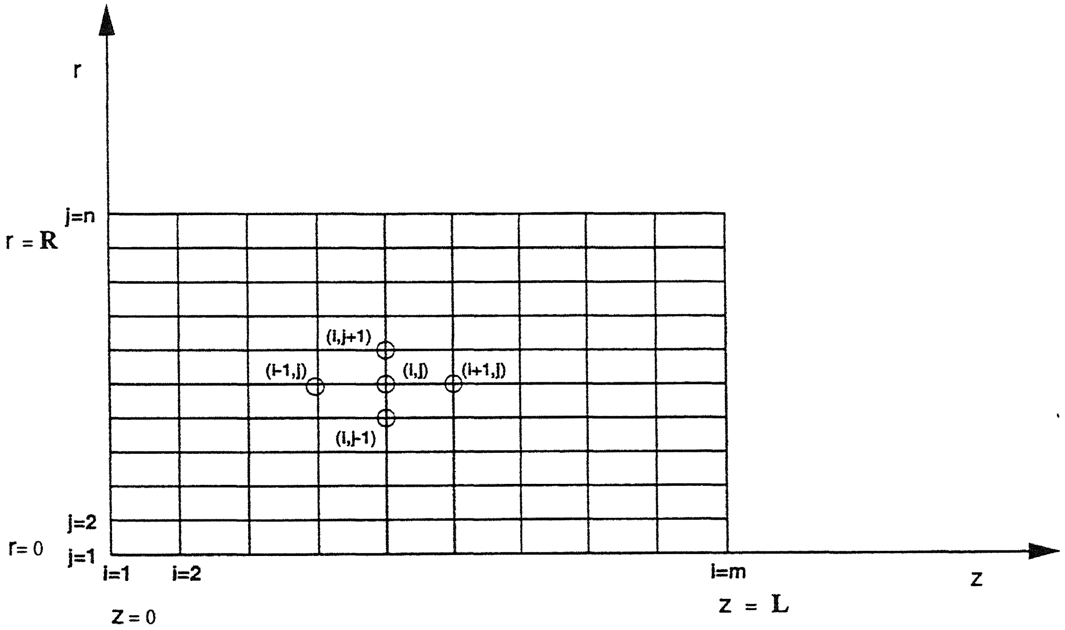

Figure 2.6: Grid for isothermal filling of cylindrical cavity at constant flow rate

Grid Point : i=1, j=1

This grid point corresponds to $r = 0$ and hence Eq.(2.12) applies here.

Since, $\frac{\partial V_z}{\partial r} = 0$, using image point technique, we have,

$$\frac{V_{z\,i,j+1} - V_{z\,i,j-1}}{2\Delta r} = 0$$

$$\Rightarrow V_{z\,i,j+1} = V_{z\,i,j-1}$$

Since, $P_{meltfront} = 0$, i.e $P_{i+1,j} = 0$

Hence, the finite difference approximation of G.D.E becomes

$$4\frac{\mu_{i,j}}{\Delta r^2}V_{z\,i,j} - 4\frac{\mu_{i,j}}{\Delta r^2}V_{z\,i,j+1} - \frac{P_{i,j}}{Z} = 0 \tag{2.14}$$

Grid Point : i=2, j=2,n-2

The finite difference approximation of the Eq.(2.13) is,

$$V_{z\,i,j-1}\left(-\frac{\mu_{i,j}}{2\Delta r\; r_{i,j}} + \frac{\mu_{i,j}}{\Delta r^2} - \frac{\mu_{i,j+1} - \mu_{i,j-1}}{4\Delta r^2}\right) + V_{z\,i,j}\left(-2\frac{\mu_{i,j}}{\Delta r^2}\right)$$

$$+V_{z\,i,j+1}\left(\frac{\mu_{i,j}}{2\Delta r\; r_{i,j}} + \frac{\mu_{i,j}}{\Delta r^2} + \frac{\mu_{i,j+1} - \mu_{i,j-1}}{4\Delta r^2}\right) + \frac{P_{i,j}}{Z} = 0 \tag{2.15}$$

Grid Point : i=2, j=n-1

The finite difference approximation of the Eq.(2.13) is,

$$V_{z\,i,j-1}\left(-\frac{\mu_{i,j}}{2\Delta r\; r_{i,j}} + \frac{\mu_{i,j}}{\Delta r^2} - \frac{\mu_{i,j+1} - \mu_{i,j-1}}{4\Delta r^2}\right)$$

$$+V_{z\,i,j}\left(-2\frac{\mu_{i,j}}{\Delta r^2}\right) + \frac{P_{i,j}}{Z} = 0 \tag{2.16}$$

2.2.4 Method of Solution

A direct solution method or implicit method has been used to solve the governing differential equation. To solve the set of linear simultaneous algebraic equations arising out of the discretization of the governing differential equation, the Thomas algorithm has been used.The correct injection pressure at a given time is obtained iteratively by Newton -Raphson method[see Appendix A]. The solution gives us injection pressure required at a particular time to achieve the desired flow rate. The accuracy of the solution depends on the grid spacing in r and z-directions. The whole algorithm for simulation of the process is shown in flow chart, Fig.2.7.

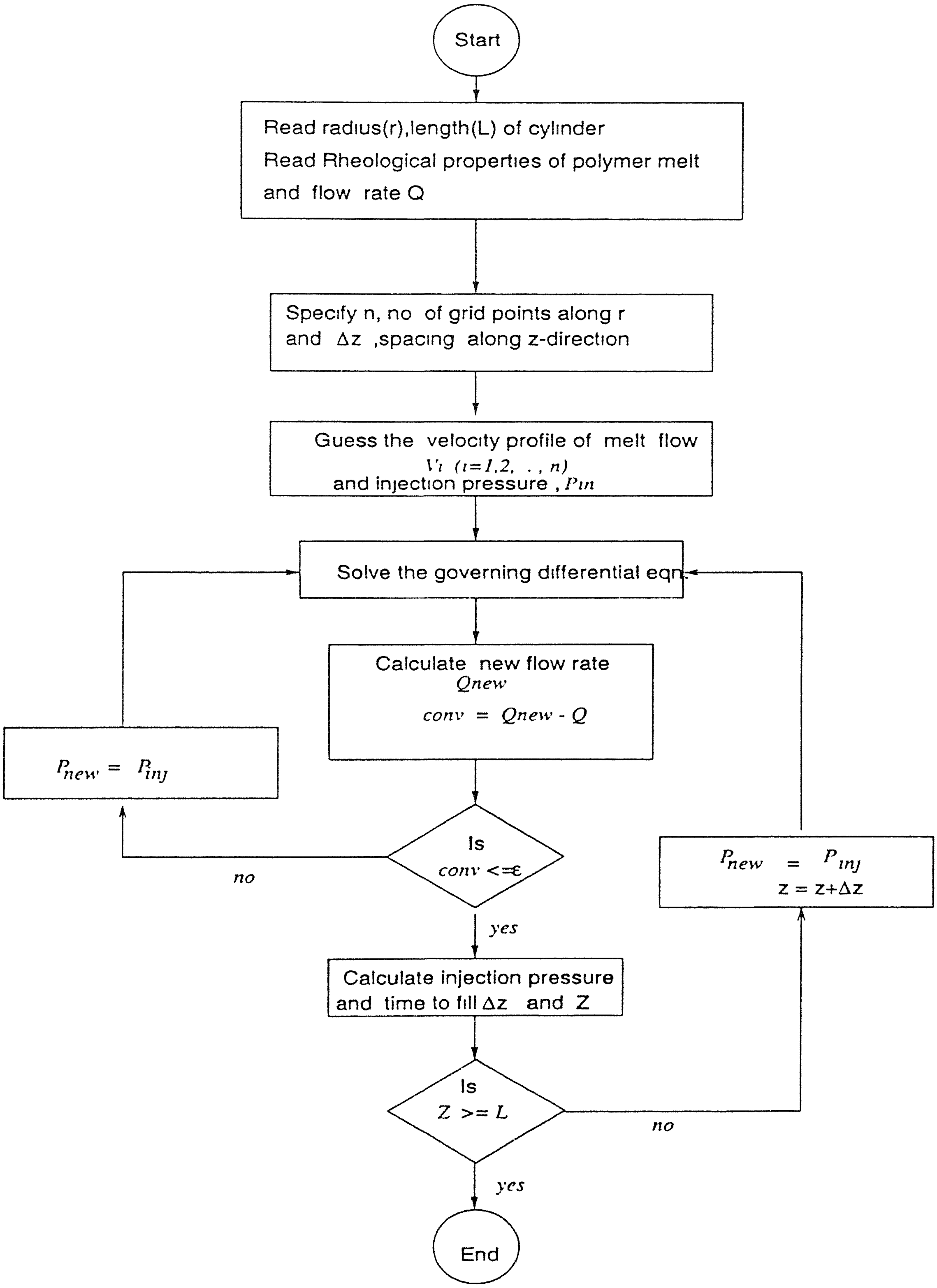
Start
Read radius(r),length(L) of cylinder
Read Rheological properties of polymer melt
and flow rate Q
Specify n, no of grid points along r
and Δz ,spacing along z-direction
Guess the velocity profile of melt flow
Vi (i=1,2, . . , n)
and injection pressure , Pin
Solve the governing differential eqn.
Calculate new flow rate
Qnew
conv = Qnew - Q
Pnew = Pinj
Is
conv <=ε
no
yes
Pnew = Pinj
z = z+Δz
Calculate injection pressure
and time to fill Δz and Z
Is
Z >= L
no
yes
End

Figure 2.7: Flow chart of algorithm to simulate the isothermal filling of cylindrical cavity at constant flow rate.

2.3 Non-Isothermal Filling of Cavity at Constant Flow Rate

2.3.1 Problem Statement

Consider the quasi-steady, fully developed, incompressible flow of polymer melt along a circular tube of length L and diameter D shown in Fig.2.1. The mould is kept at a temperature T_{mould}. The polymer melt enters at a temperature T_i, forced by a variable injection presure P_{inj} so that the flow rate Q in the cavity is constant.

2.3.2 Formulation

Cylindrical polar co-ordinates r and z are appropriate for describing the axi-symeteric flow, in which the there is no variations with respect to the third angular co-ordinate, θ and $V_\theta = 0$. Fully developed flow implies that $\frac{\partial V_z}{\partial Z} = 0$. From the equation of continuity it can be deduced that $V_r = 0$.

Since, the problem is thermally and geometrically symmetric about the longitudinal axis, only one half of the physical domain is considered. The computational domain is shown in Fig.2.8.

Governing Differential Equation:

The governing differential equations for this case are :

Energy Equation:

Neglecting axial diffusion.

$$\rho\, C_p V_z \frac{\partial T}{\partial Z} = k\, \frac{1}{r}\, \frac{\partial}{\partial r}\, (r\frac{\partial T}{\partial r}) + \mu (\frac{\partial V_z}{\partial r})^2 \tag{2.17}$$

Convection *Conduction* *Viscous dissipation*

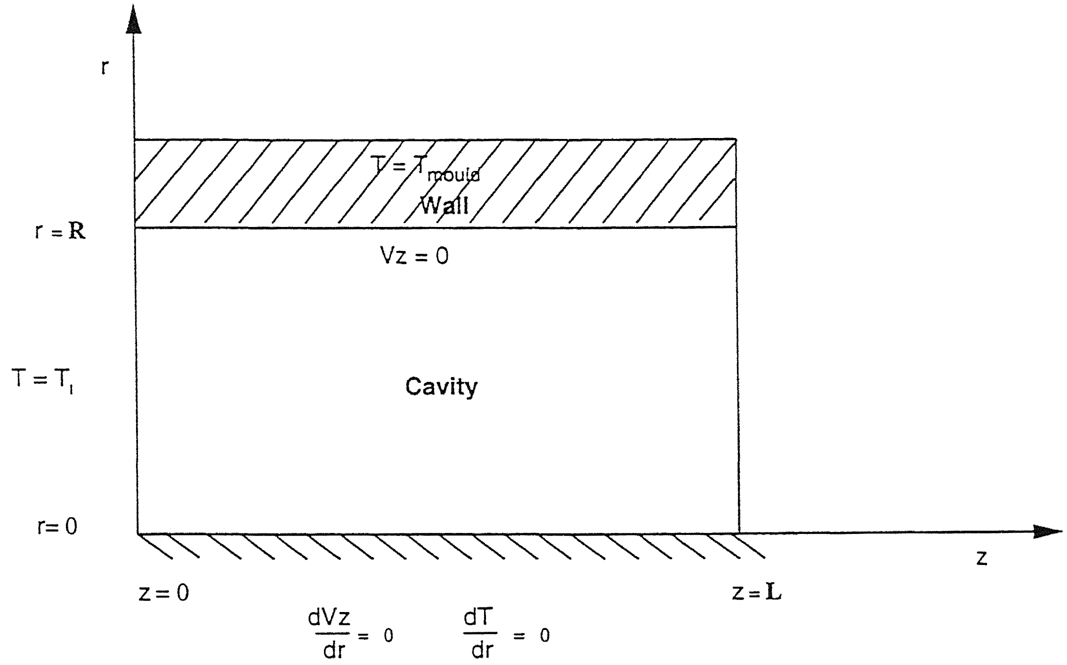

Figure 2.8: Computational domain for non-isothermal filling of cylindrical cavity.

Momentum Equation:

$$\frac{\partial P}{\partial Z} = \frac{1}{r}\frac{\partial}{\partial r}\left(r\tau_{rz}\right) \tag{2.18}$$

where,

$$\tau_{rz} = \mu \, \frac{\partial V_z}{\partial r}$$

and,

$$\mu = m\left|\frac{\partial V_z}{\partial r}\right|^{n-1} e^{-b\,(T-T_i)}$$

for Power law fluid.

Since the viscosity is dependent on the strain rate as well as temperature, the momentum and energy equations becomes coupled and need to be solved simulatenously.

Boundary Conditions:

$$B\,C.1 \quad r = 0, \frac{\partial V_z}{\partial r} = 0 (axi - symmetry)$$

$$B.C\,2 \quad r = 0, \frac{\partial T}{\partial r} = 0 \quad (axi - symmetry)$$

$$B.C.3 \quad r = R, V_z = 0 \qquad (no - slip)$$

$$B.C.4 \quad r = R, \qquad -k\frac{\partial T}{\partial r} = h(T \;-\; T_{mould})$$

$$(Heat\ transfer\ from\ melt\ to\ mould)$$

The pressure at the melt front is always zero because the atmospheric pressure prevails there, so $P_{meltfront} = 0$.

Explanation for B.C.4

Even if the thermal contact resistance between the melt and the mould cavity can be assumed negligible, an interface condition between the melt and the mould is implemented. The variation in the heat transfer at the interface is a complex phenomenon that depends on many factors such as surface roughness, geometry, mould coating, and polymer composition. From the model point of view, the interface modelling adds flexibility. It facilitates the coupling between the flow equations and the heat transfer. The condition specified at the interface is such that the heat flux must be conserved across the discontinuity. This is expressed as :

$$q = h(T_{melt} - T_{mould})$$

The melt-mould thermal contact resistance coefficient h is determined experimentally(Kamal et al., 1991). In the present work, a suitable value for h is taken as $2X10^8 W/m^2\ ^\circ C$ (Hetu et al.,1998).

2.3.3 Details of Finite Difference Formulation

Simplifying energy Eq.(2.17) we get,

For $r = 0$

$$\rho\, C_p V_z \frac{\partial T}{\partial Z} = 2k\, \frac{\partial^2 T}{\partial r^2} \tag{2.19}$$

and,

$$\mu = \mu_0\, e^{-b\,(T-T_i)}$$

whrere, μ_0 is viscosity at zero shear.

For $r > 0$

$$\rho\, C_p\, V_z \frac{\partial T}{\partial Z} = k\, (\frac{1}{r}\, \frac{\partial T}{\partial r} + \frac{\partial^2 T}{\partial r^2}) \tag{2.20}$$

and,

$$\mu = m| \frac{\partial V_z}{\partial r} |^{n-1}\, e^{-b\,(T-T_i)}$$

The energy equation is solved explicitly. The grid is shown in Fig.2.9.

Depending upon the locations of grid points two-point/three-point forward/backward/central difference schemes of first/second order of accuracy for various derivatives appearing in Eq.(2.19)and Eq.(2.20) have been used. A grid of any size can be used.

Grid Point : i=1, j=1

This grid point is subjected to boundary condition $\frac{\partial T}{\partial r} = 0$. Hence, the resulting G.D.E is

$$\rho\, C_p V_z \frac{\partial T}{\partial Z} = 2k\, \frac{\partial^2 T}{\partial r^2}$$

Since, $\frac{\partial T}{\partial r} = 0$, using image point technique, we have,

$$\frac{T_{i,j+1} - T_{i,j-1}}{2\Delta r} = 0$$

$$\Rightarrow T_{i,j+1} = T_{i,j-1}$$

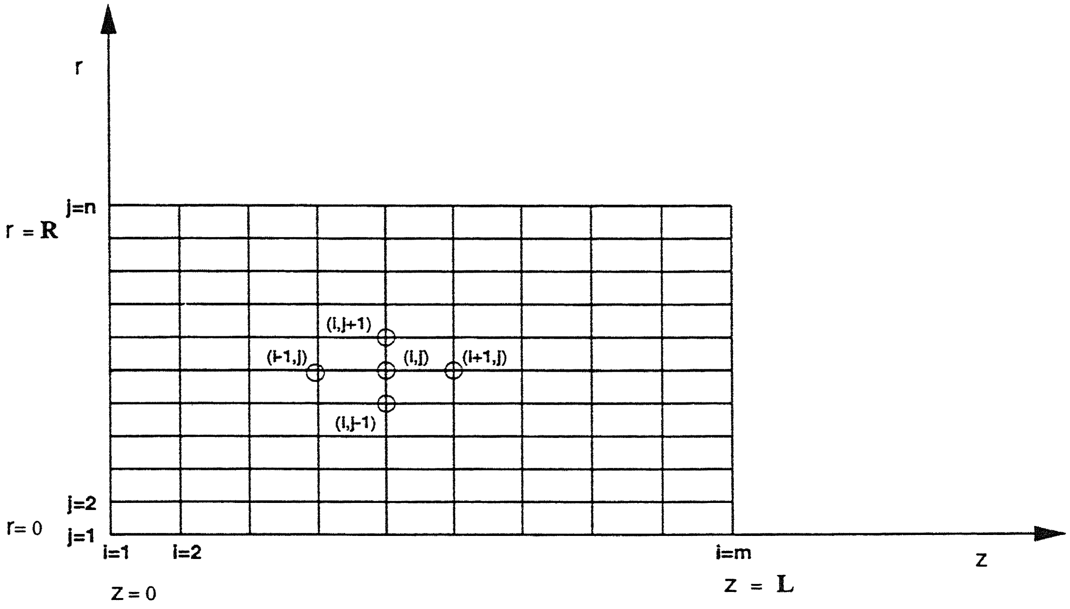

Figure 2.9: Grid for non-isothermal filling of cylindrical cavity.

Hence, the finite difference approximation of above equation is,

$$T_{i+1,j} = (1 - \frac{4\,k\,\Delta Z}{\rho\,C_P\,V_{z\,i,j}\,\Delta r^2})T_{i,j}$$

$$+ \frac{2\,k\,\Delta Z}{\rho\,C_P\,V_{z\,i,j}\,\Delta r^2}(T_{i,j+1} - T_{i,j-1}) \qquad (2.21)$$

Grid Point : i=1, j=2,n-1

For this grid point the resulting G.D.E is ,

$$\rho\,C_p V_z \frac{\partial T}{\partial Z} = k\,(\frac{1}{r}\frac{\partial T}{\partial r} + \frac{\partial^2 T}{\partial r^2})$$

Hence, the finite difference approximation of G.D.E is

$$T_{i+1,j} = (1 - \frac{2\,k\,\Delta Z}{\rho\,C_P\,V_{z\,i,j}\,\Delta r^2})T_{i,j}$$

$$+ \frac{k \, \Delta Z}{\rho \, C_P \, V_{z\, i,j}} \left(\frac{T_{i,j+1} + T_{i,j-1}}{\Delta r^2} + \frac{1}{r} \, \frac{T_{i,j+1} - T_{i,j-1}}{2 \, \Delta r} \right)$$

$$+ \frac{\mu_{i,j} \, \Delta Z}{\rho \, C_P \, V_{z\, i,j} \, \Delta r^2} \left(\frac{V_{z\, i,j+1} - V_{z\, i,j-1}}{\Delta r} \right)^2 \tag{2.22}$$

Grid Point : i=1, j=n

This grid point is subjected to boundary condition

$$-k \frac{\partial T}{\partial r} = h(T - T_{mould})$$

The finite difference approximation of this equation gives,

$$T_{i,j+1} = -\frac{2 \, h \, \Delta r}{k} (T_{i,j} - T_{mould}) + T_{i,j-1} \tag{2.23}$$

Here, $V_z = 0$ so, the resulting G.D.E for this case is

$$k \left(\frac{1}{r} \, \frac{\partial T}{\partial r} + \frac{\partial^2 T}{\partial r^2} \right) = 0$$

The finite difference approximation of this equation gives,

$$T_{i,j} = \frac{\frac{1}{2}(\frac{1}{r} + \frac{1}{\Delta r})(\frac{2\, h\, \Delta r}{k}) T_{mould} + \frac{2}{\Delta r} T_{i,j-1}}{(1 + \frac{2\, h\, \Delta r}{k})} \tag{2.24}$$

Here, $T_{i,j}$ at next z-increment is calculated using the previously calculated value of $T_{i,j-1}$ at that z-increment(using Eq.(2.22)).

The discretization of the momentum equation is shown in the previous articles of this chapter.

2.3.4 Average Melt Temperature

Once the temperature profile at any z-location is obtained, the average melt temperature is calculated using the concept of mixing-cup tempetaure(Holman,1997) as shown below.

$$T_{avg} = \frac{\int_0^R 2\pi r dr\ \rho V_z\ C_p\ T}{\int_0^R 2\pi r dr\ \rho V_z\ C_p} \tag{2.25}$$

The trapezoidal rule is used to calculate the integeral.

2.3.5 Stability Criterion

Since the energy equation is parabolic in z-direction the following restriction regarding ΔZ has to be imposed in order to obtain stable solution by explicit method.

For $r = 0$

$$\Delta Z \leq \frac{\rho\ C_P\ V_{z\ i,j}\ \Delta r^2}{4\ k} \tag{2.26}$$

For $r > 0$

$$\Delta Z \leq \frac{\rho\ C_P\ V_{z\ i,j}\ \Delta r^2}{2\ k} \tag{2.27}$$

To obtain the stable solution the smallest of two $\Delta Z'$s should be taken.

2.3.6 Method of Solution

Due to high temperature sensitivity of the polymer melt viscosity, the accuracy of temperature distribution plays a crucial role in a realistic simulation of the injection moulding process. In the present formulation, an explicit scheme has been used to solve the energy equation, which is parabolic in $z-$direction and hence the $z-$coordinate behaves like a time co-ordinate A numerical stability criterion has been used to check the stability. Once the temperature field within the computational domain is known at a given instant(or $z-$direction), the flow field and corresponding velocity distribution and injection pressure at a particular instant(or $z-$direction) can be determined by solving the momentum equation as discusssed in the previous sections. The accuracy of the solution depends on the grid spacing in the $r-$direction and the space increment in $z-$direction. The overall algorithm for simulation of this process is shown in flow chart depicted in Fig.2.10.

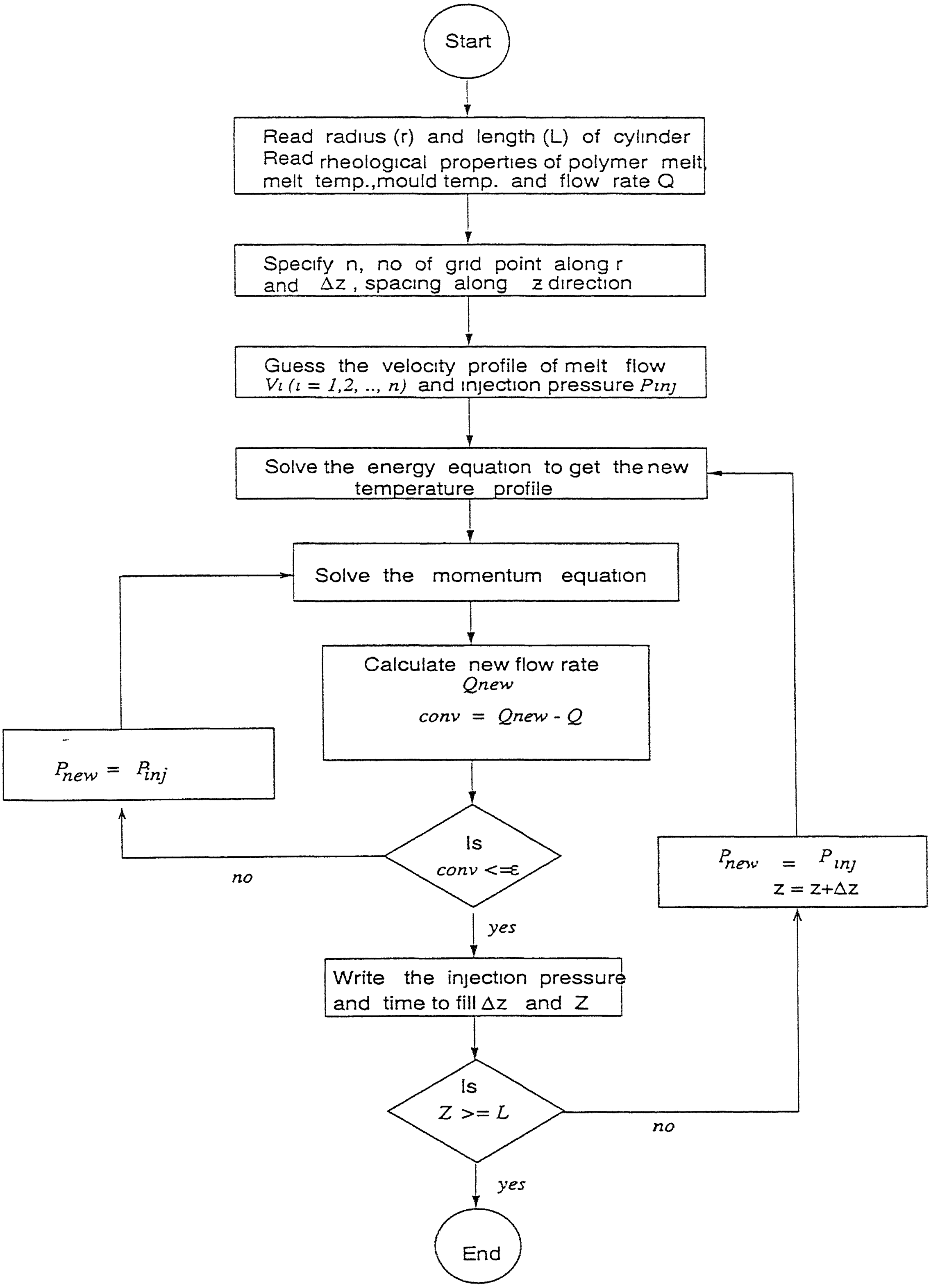
Start
Read radius (r) and length (L) of cylinder
Read rheological properties of polymer melt
melt temp.,mould temp. and flow rate Q
Specify n, no of grid point along r
and Δz , spacing along z direction
Guess the velocity profile of melt flow
Vi (i = 1,2, .., n) and injection pressure Pinj
Solve the energy equation to get the new temperature profile
Solve the momentum equation
Calculate new flow rate
Qnew
conv = Qnew - Q
Pnew = Pinj
Is
conv <=ε
no
yes
Pnew = Pinj
z = z+Δz
Write the injection pressure
and time to fill Δz and Z
Is
Z >= L
no
yes
End

Figure 2.10: FLow chart of algorithm to simulate the non-isothermal filling of cylindrical cavity.

Chapter 3

RESULTS AND DISCUSSION

Mould filling simulation requires the calculation of the detailed velocity and temperature profiles throughout the mould flow region, including the position and shape of the advancing front. This helps the analyst to determine orientation distribution affecting the article morphology, which evolves upon cooling and solidification. Such a model will facilitate the theoretical mould design as well as optimizing moulding conditions for specific property requirements.

In the present study three cases of mould flow in a circular cavity of length 25.4 cm (.254 m) and radius 2.54mm ($2.54X10^{-3}$ m) have been considered. They are (i) Isothermal constant injection pressure (ii) Isothermal constant flow rate (iii) Non-isothermal constant flow rate. The results have been shown for LDPE(low density polyethylene) following power law model of viscosity. It may be noted that when the ratio of the heat generated by viscous dissipation to that lost by heat transfer to cold walls is close to unity, fair estimates of filling time can be obtained by assuming isothermal flow(Tadmor and Gogos, 1979). For isothermal cases a grid of 101 X 101 has been used. For non-isothermal case a grid of 31 X 181 has been used. All computations have been carried out on HP-9000 computer system at IIT Kanpur.

3.1 CASE I : Isothermal Filling : Constant Injection Pressure

The input data for this case are shown in Table 3.1. Values of Z and Q are listed for various times in Table 3.2. The excellent match with corresponding analytical solution(Tadmor and Gogos. 1979) shows the correctness of the numerical solution.

These results clearly indicate that we should expect a very high flow rate and quick filling intially, followed by a rapid drop in Q and long filling times for the remainder of the long cavity. Fig.3.1 shows the Z Vs. t curve for the present numerical solution. It is clear that $\frac{\partial Z}{\partial t}$ is high in the beginning whereas with increasing time $\frac{\partial Z}{\partial t}$ drops off rapidly. This is obvious because with increasing Z, Q decreases at a fast rate. Fig.3.2 shows the flow rate Q Vs. Z. It essentially reproduces Table 3.2 in graphical form.

Fig.3.3 depicts the half melt velocity profile at various z-locations indicated by percent filling distance. It is clear that the profile is intially parabolic but turns to flat as the cavity is filled more and more. Thus the shape of the melt front flattens out with increasing axial distance. It is also seen that the magnitude of the maximum velocity(located at the centre axis) decreases with increasing Z.

Table 3.1: Input Data for Case I(Tadmor and Gogos,1979)

m	$9360(N\ s^n/m^2)$
n	0.41
P_{inj}	15.6 (MPa)
T_i	$160°C$
μ_0	$6300(N\ s/m^2)$

Table 3.2: Values of t and Q at various Z

Z	t_{anal}	t_{numl}	Q_{anal}	Q_{numl}
0 035	$1.00X10^{-3}$	$.97X10^{-3}$	$.207X10^{-3}$	$217X10^{-3}$
0 106	$.169X10^{-1}$	$143X10^{-1}$	$.359X10^{-5}$	$.437X10^{-5}$
0.150	.147	.146	$.601X10^{-5}$	$.606X10^{-5}$
0.200	394	.391	$.298X10^{-5}$	$.302X10^{-5}$
0.250	.850	.847	$.173X10^{-5}$	$174X10^{-5}$
0.254	.897	.893	$.166X10^{-5}$	$.168X10^{-5}$

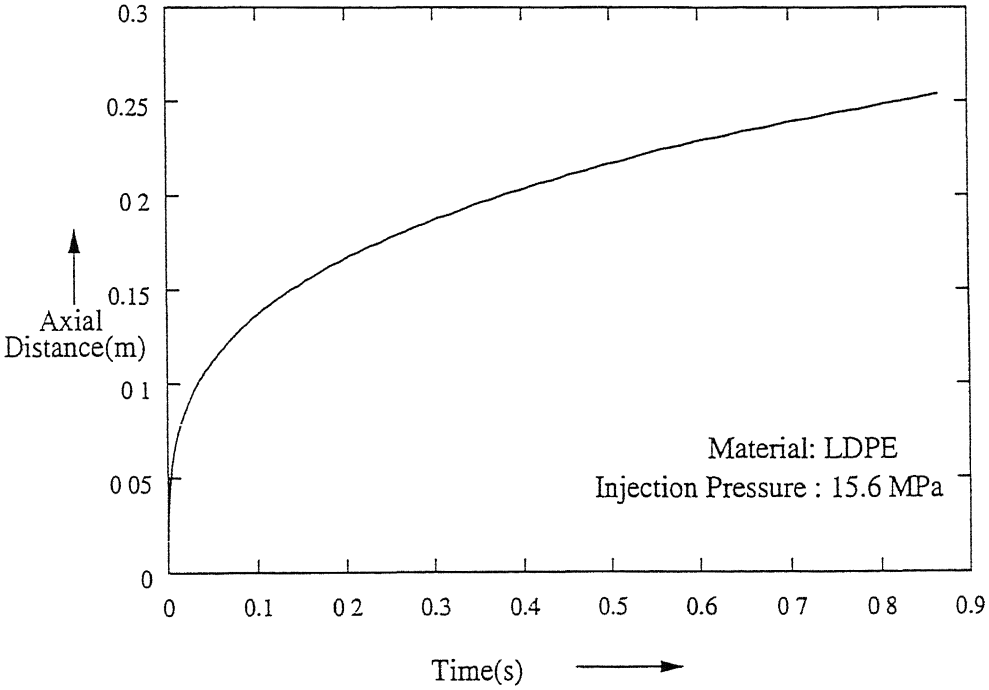

Figure 3.1: Position of advancing melt front as a function of time for constant injection pressure isothermal filling.

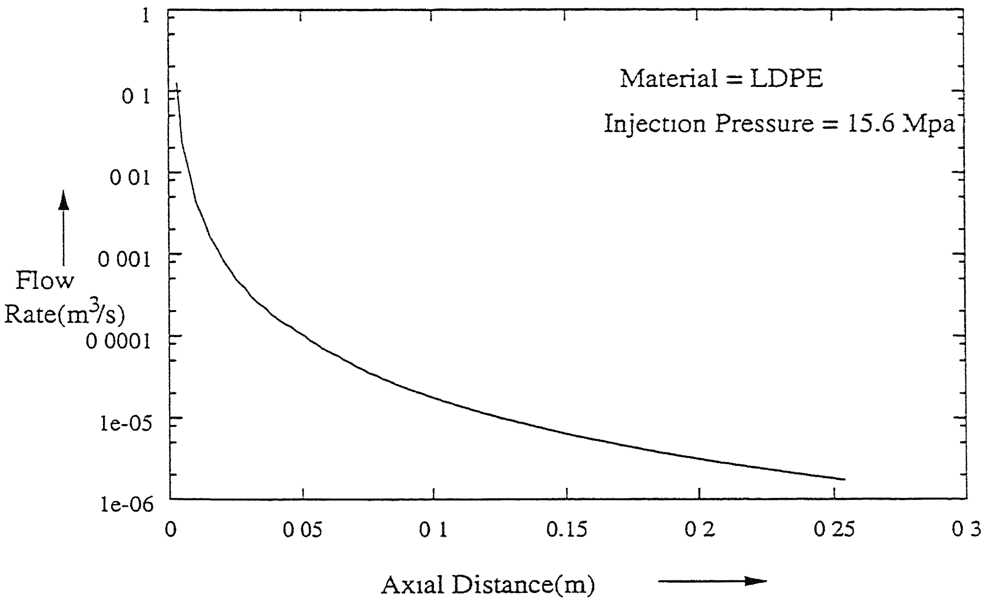

Figure 3.2: Flow rate versus axial distance for constant injection pressure isothermal filling.

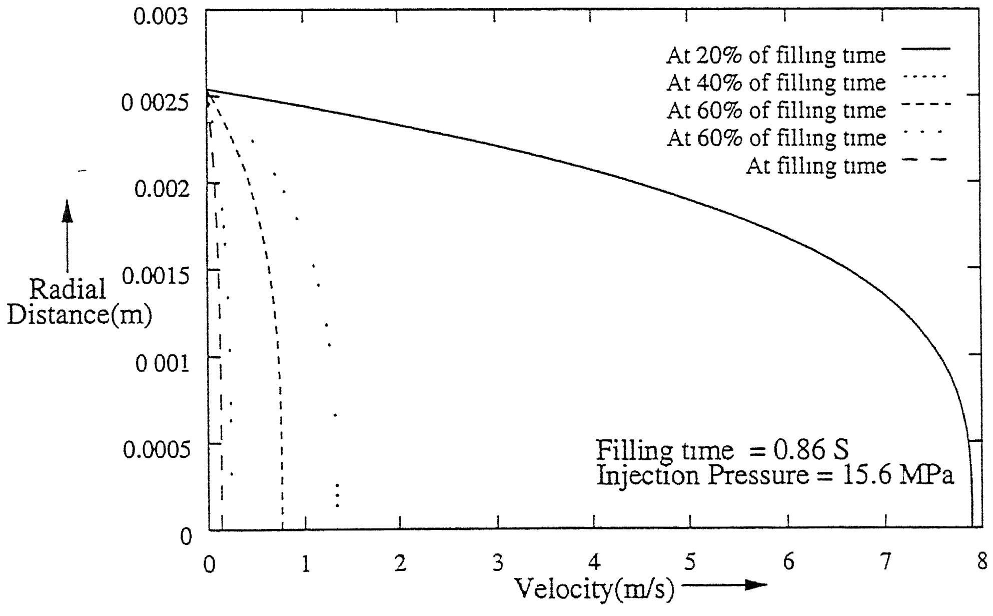

Figure 3.3: Melt velocity profile at various Z-locations for constant injection pressure isothermal filling.

3.2 CASE II: Isothermal Filling : Constant Flow Rate

The input data for this case are shown in Table 3.3. Fig.3.4 shows the plot of injection pressure versus time. It is observed that an applied pressure linearly

Table 3.3: Input Data for Case II(Tadmor and Gogos.1979)

m	$9360(N\ s^n/m^2)$
n	0.41
Q	$.515X10^{-2}\ (m^3/s)$
T_i	$160°C$
μ_0	$6300(N\ s/m^2)$

Table 3.4: Comparison of $P_{inj,anal}$ and $P_{inj,numl.}$ Vs t

t (S)	$P_{inj,anal}$ (MPa)	$P_{inj,numl.}$ (MPa)
$.100X10^{-3}$	124.34	125.61
$.500X10^{-3}$	629.05	626.23
$600X10^{-3}$	753.54	754.86
$.700X10^{-3}$	880.67	880.67
$.800X10^{-3}$	1004.48	1006.82
$.900X10^{-3}$	1133.29	1132.15
$.100X10^{-2}$	1259.32	1258.10

increasing with time is required. This is because with time the melt tends to slow down and therefore, to maintain the constant flow rate, the injection pressure is continuously increased. This linear trend can be easily justified from the analytical solution(Tadmor and Gogos, 1979) for $Q(t)$ which is given as:

$$Q(t) = \frac{\pi R^3}{s+3}\left(\frac{RP_{inj}}{2\,m\,Z(t)}\right)^s$$

If $Q(t)$ is constant, then P_{inj} must be linearly proportional to $Z(t)$ since $R.m,s(=\frac{1}{n})$ are constants. Table 3.4 shows a comparison of injection pressure versus time between the present and analytical solution. The tally is excellent. In actual practice. variable injection pressure case is more common since it is easy to implement and has a better control over the filling time.

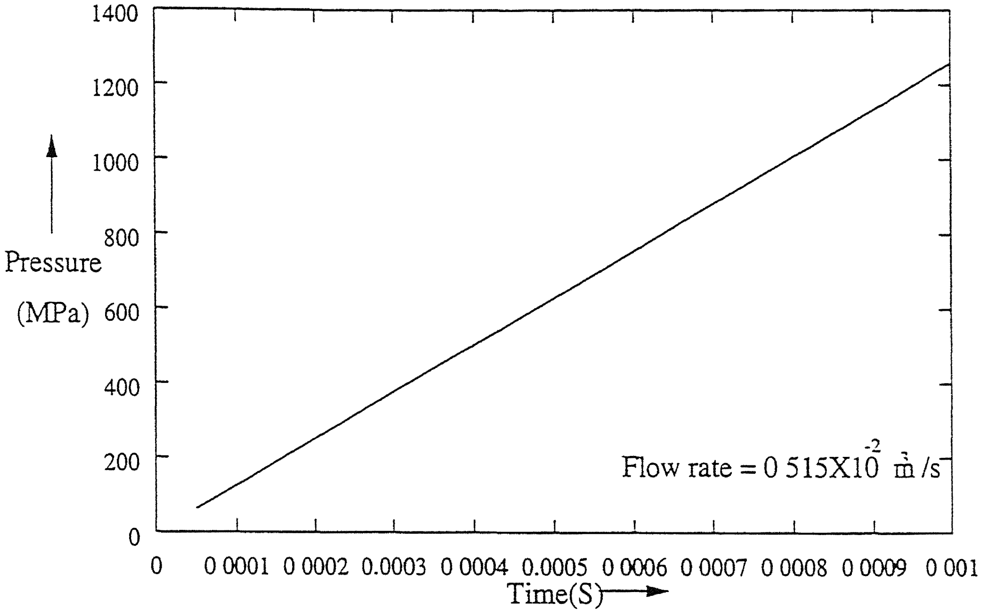

Figure 3.4: Plot of injection pressure versus time for constant flow rate isothermal filling

3.3 CASE III: Non-Isothermal Filling : Constant Flow Rate

In practial situations, isothermal filling is difficult to achieve. Therefore, we turn our attention to the scenario where the mould is kept at fixed temperature and the melt is losing heat to the mould. The input data for this case are shown in Table 3.5.

Fig.3.5 shows a comparison of injection pressure versus time for non-isothermal and isothermal filling. It is evident that the injection pressure increases nonlinearly with time for the non-isothermal filling. This is in sharp contrast with isothermal filling which requires injection pressure to be increased linearly with time. This is because of the fact that in tha case of non-isothermal filling momentum equation is coupled with the energy equation through the viscosity which is a function of strain rate as well as temperature. Also, it is seen that the requirement of injection pressure rise with time is much less in case of non-isothermal filling because of the effect of viscous heat generation in

Table 3.5: Input Data for Case III

m	$9360(N\ s^n/m^2)$
n	0.41
b	$0.01\ (°C^{-1})$
ρ	$525(kg/m^3)$
C_p	$2300(J/kg°C)$
k	$0.335(W/m°C)$
h	$2X10^8(W/m^2\ °C)$
μ_0	$6300(N\ s/m^2)$
T_i	$200°C$
T_{mould}	$60°C$
Mould Material	*Steel*

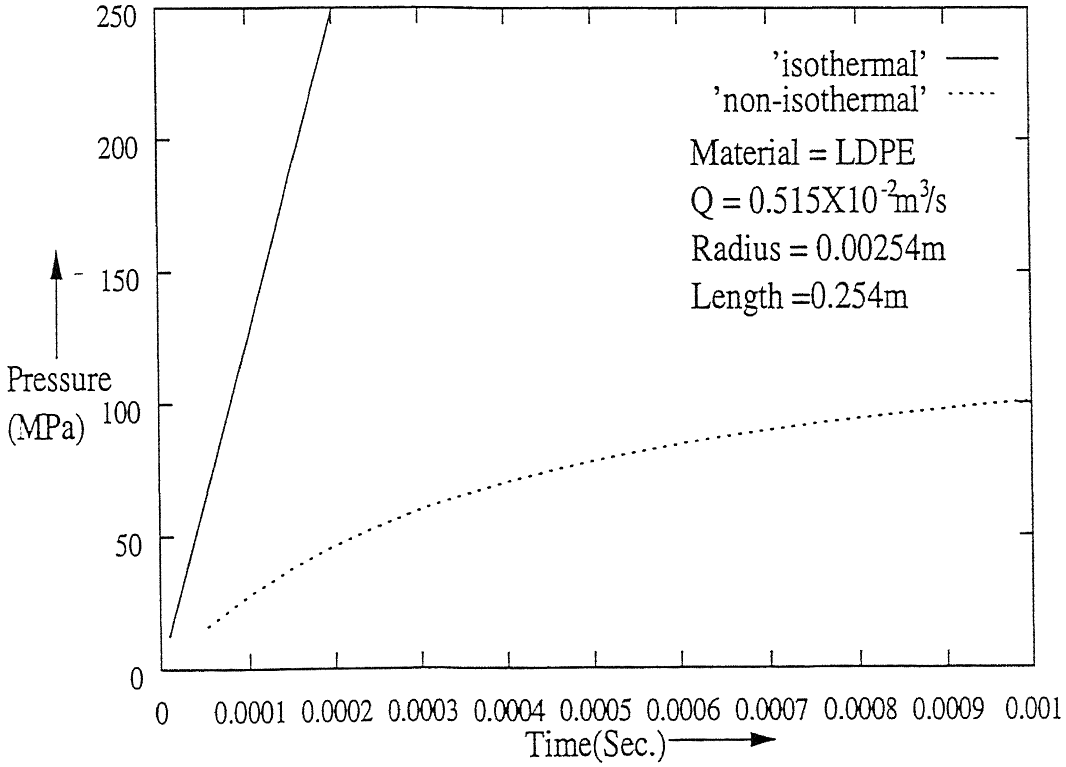

Figure 3.5: Comparison of injection pressure versus time for non-isothermal and isothermal filling at constant flow rate.

the melt which raises the temperature and hence decreases the viscosity of the melt. As a result, less injection pressure is required to push the melt through the cavity. The viscosity decreases more towards the end of the cavity due to higher average temperature and hence $\frac{\partial P_{inj}}{\partial t}$ also decreases thus producing a flatter curve as the time increases. However, this trend is valid for high flow rate case which applies here.

Fig.3.6 shows the melt temperature field at various z-locations for $Q = .515X10^{-4}\ m^3/s$. The layer near the centre is virtually isothermal throughout filling, which is due to the fact that the velocity gradients are zero and the thermal conductivity of the melt is low . As one approaches the wall of the cavity, the temperature increases with radial position, it goes through a maximum and then decreases to low values. The maximum is a result of the competition between the viscous heat dissipation and heat conduction The level of the largest maximum is nearly $238°C$. As stated above, the temperature rapidly drops at larger radial positions. This is due to the fact that in this region the melt has resided in the cold cavity, and near the wall, for a longer period of time.

Fig.3.7 shows the same plots as in Fig.3.6 but for $Q = .107X10^{-4}\ m^3/s$ that is for a much lower flow rate. It is interesting to see that no peak appears in this case. The average temperature at 80% of filling is lower than that at 20% of filling which means that the temperature of the melt decreases as it flows towards the end of the cavity. This is because of the fact that at low flow rates the velocity profile is flatter and hence viscous dissipation is less and therefore, the maximum temperature is not encountered. The reason why the melt becomes colder as it reaches the end is due to the high residence time in the cavity arising out of low flow rate and greater loss of heat to the cold mould.

From Fig.3.6 it is observed that very near the wall the temperature of the melt is below $180°C$, where the viscosity of LDPE is so high that the fluid exhibits virtually no flow. Thus, for the above regions a "frozen skin" layer is formed during filling. This layer is seen to form much earlier for lower flow rate case(Fig.3.7) that is, near $r = 0.002m$.

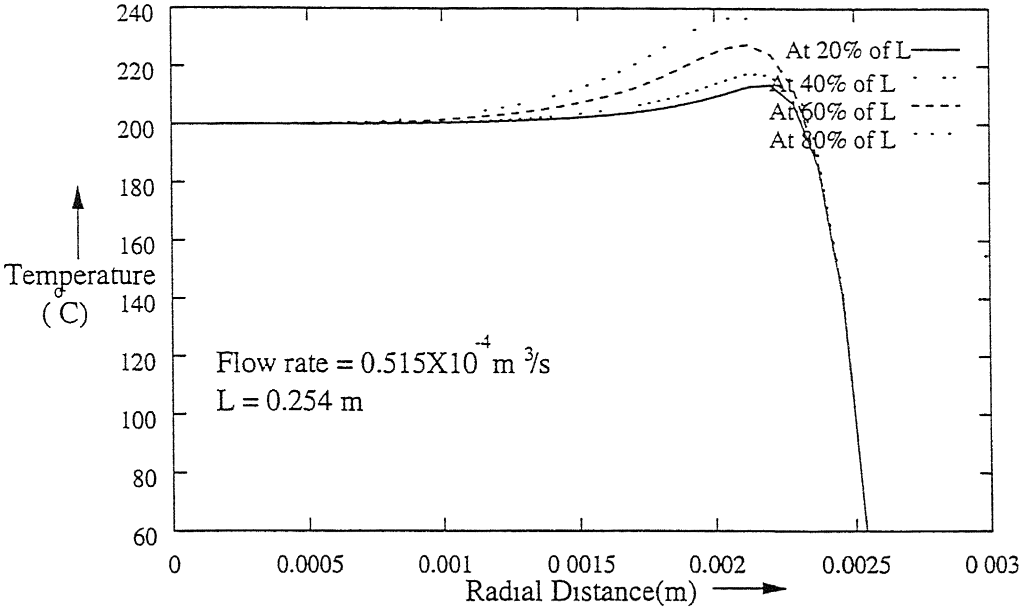

Figure 3.6: Melt temperature fields at various z-locations for $Q = 0.515X10^{-4}$ (m^3/s).

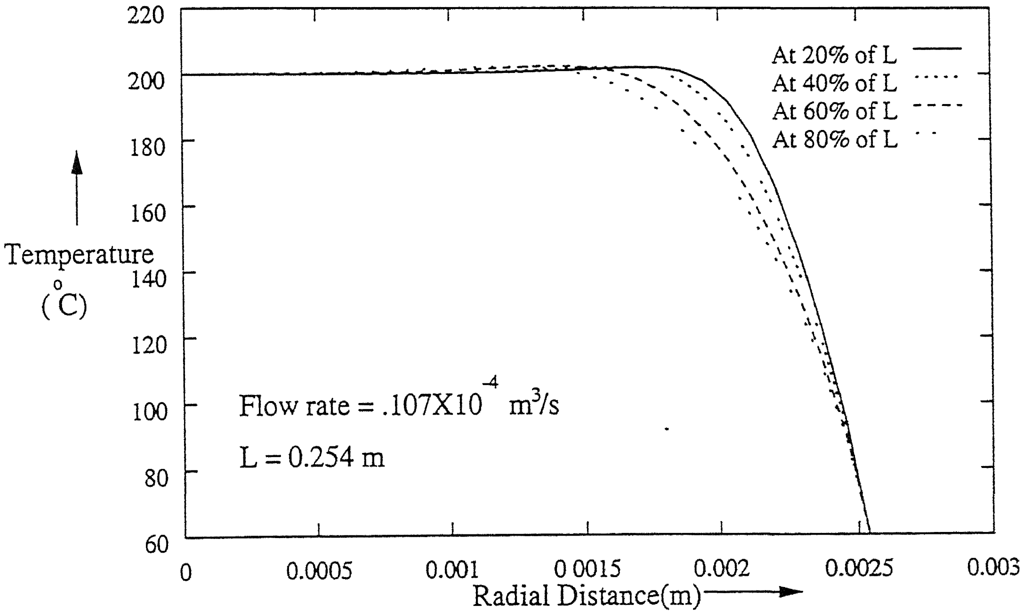

Figure 3.7: Melt temperature fields at various z-locations for $Q = 0.107X10^{-4}$ (m^3/s).

Fig.3.8 shows the frozen layer is smallest for the highest flow rate and vice-versa. The "frozen skin" layer is not desirable in that it contributes to the "moulded in" strains in the moulded article. The frozen layer can be effectively reduced or eliminated by higher injection pressure(resulting in higher flow rate), melt temperature and to a lesser but appreciable, degree by increasing mould temperature.

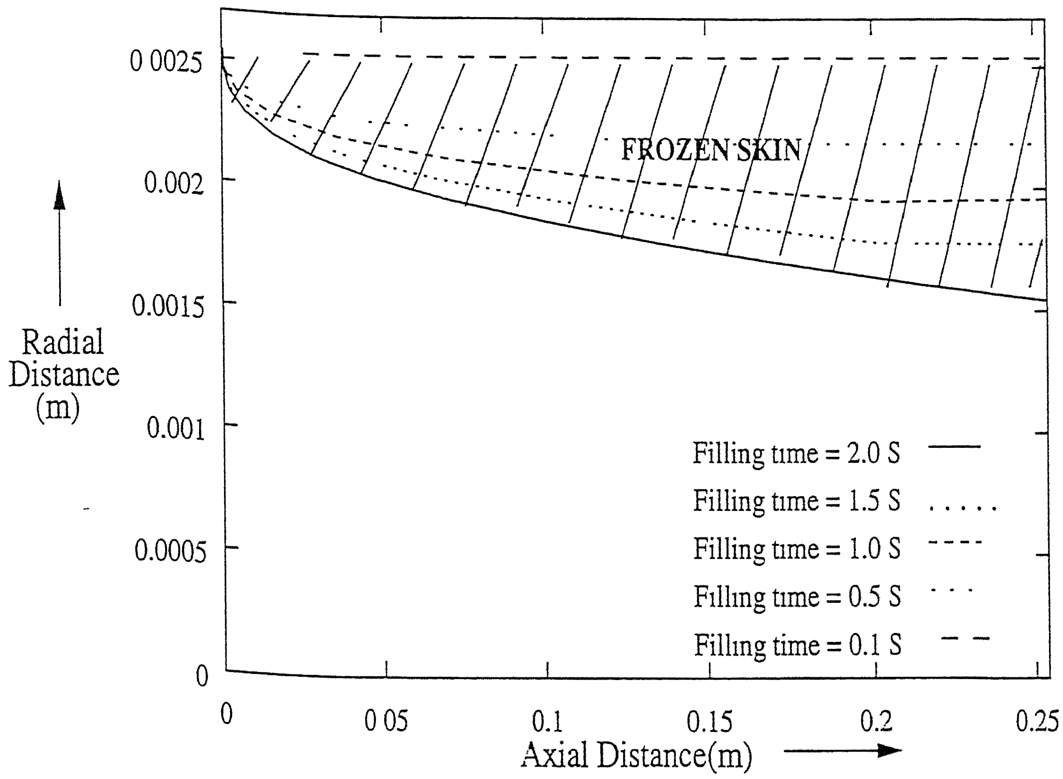

Figure 3.8: "Frozen skin" layer for various flow rates.

Fig.3.9 shows the pressure distribution in the cavity after filling. As expected. the P vs Z profile is linear with negative pressure gradient.

Fig.3 10 shows the shape of the melt front at various times. The shape of the melt front remains same throughout the filling because of constant flow rate.

It may be noted that for non-isothermal filling situation, the experimental validation could not be done because the facility for carrying out an injection moulding study experimentally is not available at IIT Kanpur. However. using the C-MOLD 3DQUICKFILL software which uses FEM formulation. the trends of the results were checked and found satisfactory.

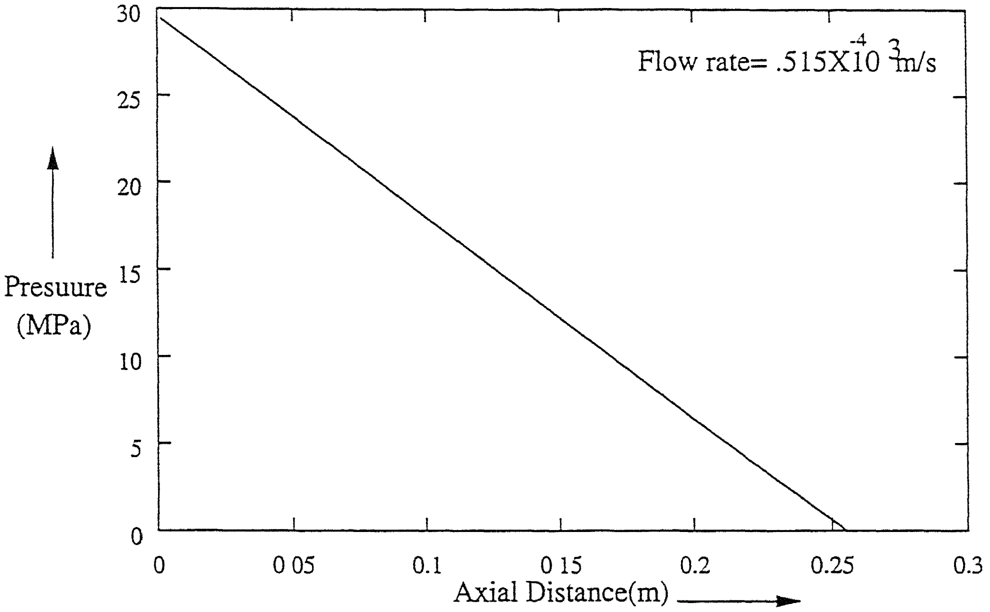

Figure 3.9: `Pressure distribution in the cavity after filling.

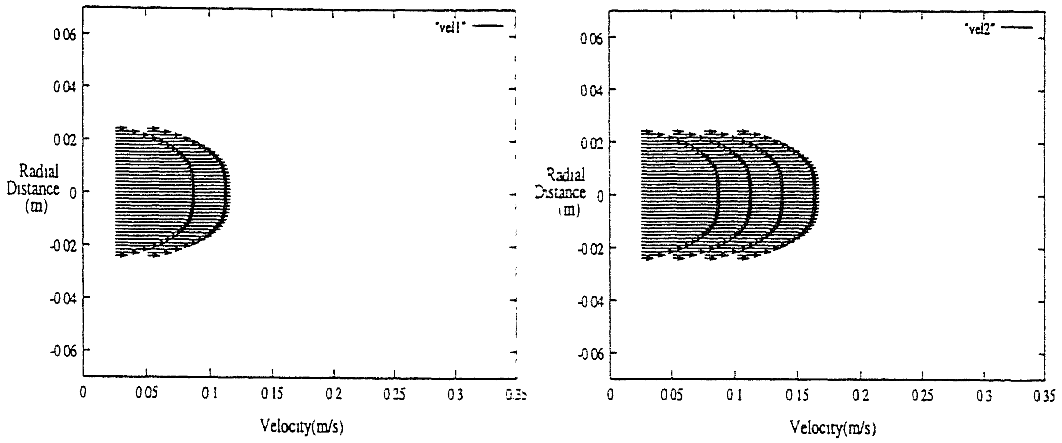

Velovity Profile after 2.0% filling of cylindrical cavity

Velovity Profile after 4.0% filling of cylindrical cavity

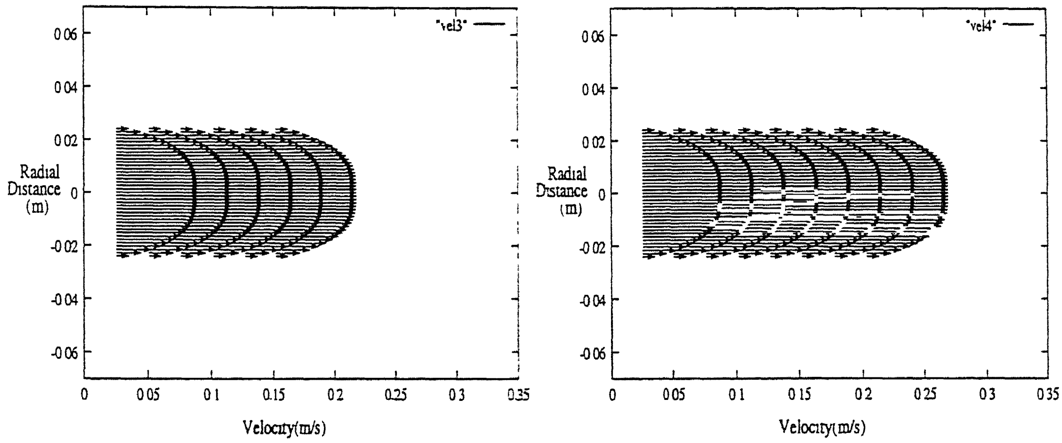

Velovity Profile after 6.0% filling of cylindrical cavity

Velovity Profile after 8.0% filling of cylindrical cavity

Filling Time= 6 s

Radius = 0.00254 m

Length = 0.254 m

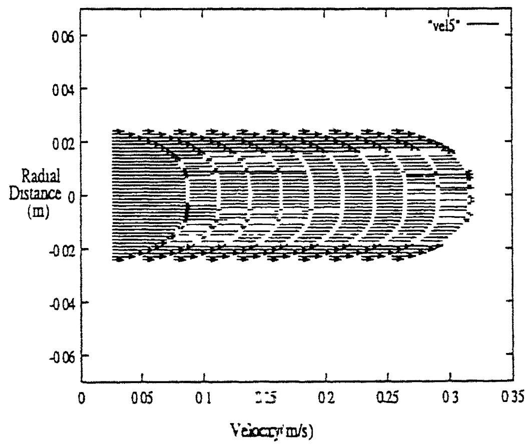

Velovity Profile after 10.0% filling of cylindrical cavity

Figure 3.10: Shape and location of the melt front at various times.

Chapter 4

OPTIMIZATION OF MOULDING CONDITIONS AND MATERIAL SELECTION

Injection moulding process is a complex but highly efficient means of producing a large variety of thermoplastic products particularly those with high production requirements, tight tolerances and complex shapes. The final product quality of injection moulded part must include final material properties as well as structural and aesthetic considerations.

The product quality is a function of the material used, the mould design and the processing conditions. The most important processing conditions during the filling phase are the mould temperature, melt temperature and filling time.

The selection of appropriate moulding conditions in the injection moulding process is a non-trivial task. We can feel the complexity by quick examination of the general effect of each variable. An increase in melt temperature causes a decrease in melt viscosity, which results in reduced pressure requirements and reduced stresses. On the other hand, high melt temperature may increase the possiblity of material burning and will also increase cooling time. Increasing the mould temerature reduces heat losses, and the maximum temperature difference at the end of the filling phase may be reduced. However, a high mould temperature increases cooling time. Short fill time require higher pressure because of higher flow rate requirement, resulting in higher shear stresses and shear rate. Then, if the fill times are too long, pressure will increase because the plastic temperature decreases and the viscosity increases It is clear from above discussion that some optimization to balance the conflicting processing parameters is required to produce a good quality product.Here, a suitable material for a particular geometry is also required to be found out

4.1 Characteristics of Process

A number of process parameters affect the formation of moulded part. The most important of them are

1. Pressure
2. Temperature
3. Time

We will discuss the effeect of presure and temperature in article 4.2.

The time for one single run usually is called the cycle time. The cycle time consists of dead time, filling time and cooling time. The faster rate of filling and cooling time decreases the cycle time which will increase the production rate. For this the cooling system must provide the most uniform possible temperature distribution in the mould so that cooling is uniform and homogeneity in micro structure results.

4.2 Quality Measures

For optimization of process parameters it is required to develop the quantitative measures of the part quality as our ultimate aim in optimizing is part quality. The term 'quality' may be referred to many product properties such as mechanical, thermal, electrical, optical or geometrical properties.

There are two type of quality measures: direct and indirect. A model that predicts the warpage from flow simulation results would be characterized as direct quality measure. An indirect quality measure of quality is a quantity that is correlated but does not produce a direct estimate of that quality. However. direct quality measures although invaluable at final stages of design process are usually more expensive and time consuming. So, an alternative method is required to be developed. Instead of using finite element stress and thermal analysis to predict warpage and material degradation directly we will discuss the determination of indirect part quality measure based on flow simulation results.

The indirect quality measures used here are those related to warpage and material degradation. We quantify the major causes of warpage and material degradation. Warpage occurs (Pandelidis and Zou, 1990) because of:

1. Uneven temperature distribution and uneven cooling in the part.
2. Inhomogeneity of part density.
3. Anisotropy in thermal shrinkage.
4. High unbalanced residual stress distribution.

The major causes of material degradation are high temperature(burning temperature) and high shear rate.

For optimization, here only those quality measures which are controllable at the filling phase are considered. The packing and cooling phase must also be considered when full design is implemented. Here, cooling time is also considered which is calculated by the equation of Bernhardt(1962)[see Appendix B].

4.2.1 Temperature Difference

Temperature difference is a measure of temperature distribution uniformity at the end of the filling stage. The temperature used here is the average temperature. The amount of shrinkage a plastic undergoes is a function of its temperature. All other factors being equal, a non-uniform temperature distribution will cause differential shrinkage and therefore, warpage in the cooling process. Heating occurs in the flow because of frictional and shearing effects. At the same time, cooling takes place at the plastic mould interface. Thus, in general, at the end of the fill stage there will be a non-isothermal temperature distribution throughout the part. In a finite difference simulation, there will be discrete temperature differential. The subsequent differential shrinkage that occurs will induce residual stresses causing warpage and other detrimental short and long -term effects.

Now the parameter T_d has been defined to quantify the severity of the temperature difference. T_d is simply the difference between the maximum and minimum temperature at the end of fill over entire part which are available in flow simulation results.

It can be shown mathematically as :

$$T_d = T_{max} - T_{min} \tag{4.1}$$

where,

T_{max} = maximum temperature in the mould
T_{min} = minimum temperature in the mould

By putting this term in the objective function differential shrinkage due to non-uniform temperature distribution can be taken into account.

4.2.2 Pressure

Another cause of warpage is non-uniform pressure distribution. During the cooling phase the areas with relatively high pressure will shrink less than areas of lower pressure.

There will be pressure losses during the filling stage. These losses are the result of the continual shearing and friction that occurs as the polymer melt is forced into the mould. Ideal conditions will exist if in each part of the mould has the same pressure gradient. However, in case of flow in axi-symmetric bodies the pressure gradient throughout is same. But higher pressure will result in higher shear rate and shear stresses which will cause warpage, mechanical sticking and flash(Bown, 1979).

The parameter P_{max} has been defined to quantify the severity of pressure distribution. By putting this term in objective function the problem of mechanical sticking and flash can be taken into account.

4.3 The Basic Method of Optimization

To solve the optimization problem a methodology is presented here. The optimization problem can be broken into three parts. An approximate feasible moulding space(AFMS) is first determined to constrain the search space for the optimization algorithm. Quality is quantified as a function of flow simulation outputs and constitutes the objective function that must be minimized. The resulting optimization problem is solved by an exhaustive search in the constrained space.

4.3.1 Determination of Approximate Feasible Moulding Space (AFMS)

To determine the AFMS, the recommended mould temperature and melt temperature range scan be obtained directly from the material database for the specific material. According to the pressure and temperature relations eight boundary moulding conditions can be defined by scanning the fill time. These eight boundary points determine eight half spaces, the intersection of which define the AFMS for the part.

Flow simulation program can be called iteratively for the different combinations of melt and mould temperature. For each combination , the program scans the fill time to determine its minimum and maximum boundaries. Eight boundary moulding conditions can be determined by applying constraints of maximum pressure and temperature distribution. These boundary moulding conditions define the AFMS.

4.3.2 Material Selection Based on AFMS

To select the appropriate material for a part, a designer first consider the chemical, physical and mechanical properties of the material which satisfy the design criteria. There may be cases when several different materials can meet the design requirements. To select the appropriate material an injection mouldability index(IMI) is defined. This is defined as

$$IMI = \int_{t_{min}}^{t_{max}} \int_{T_{mould\ min}}^{T_{mould\ max}} \int_{T_{melt\ min}}^{T_{melt\ max}} dT_{melt} dT_{mould}\ dt \qquad (4.2)$$

A small IMI implies that there may be difficulties with controlling the process on line, because of restricted range of operating conditions. Therefore, if all the considerations are equal, the material which allows for a large IMI is preferable.

4.3.3 Optimization of Moulding Conditions

Considering the quality measures and cycle time we can construct the objective function, $F(x)$ so that we can get process parameters which will result in maximum productivity with good quality product.

The function $F(x)$, has to be minimized so as to obtain optimal combination of temperature, pressure and time.

Minimize

$$F(x) = \omega_1 T_d + \omega_2 t_{cycle} + \omega_3 P_{max} \tag{4.3}$$

subject to

$$P_{max} - P_{mc} \leq 0 \tag{4.4}$$

$$T_d - T_d^a \leq 0 \tag{4.5}$$

$$X_1^l \leq X_1 \leq X_1^u \tag{4.6}$$

$$X_2^l \leq X_2 \leq X_2^u \tag{4.7}$$

$$X_3^l \leq X_3 \leq X_3^u \tag{4.8}$$

where, $X = [X_1, X_2, X_3]$ are design variables; mould temperature, melt temperature and filling time. $X_i^l (i = 1, 2, 3)$ are lowest allowable mould temperature, melt temperature and fill time and $X_i^u (i = 1, 2, 3)$ are the highest allowable mould temperature, melt temperature and filling time. And $\omega = [\omega_1, \omega_2, \omega_3]$ are the weights of design variables.

The above optimization problem is solved using exhaustive search in the AFMS. Since, the geometry of mould is simple, this method has been used.

4.4 Results

The problem of non-isothermal filling of the cylindrical mould and subsequent cooling is being investigated here. The problem of filling has been described in article 2.3. For the cooling the equation given by Bernhardt(1962)[see Appendix B] is used.

Input Data:

Length : 0.254 m

Diameter : 0.00254 m

Material : LDPE

Mould Temperature range : $60°C - 80°C$

Melt Temperature range : $200°C - 240°C$

First the mould temperature and melt temperature is chosen as $60°C$ and $200°C$ respectively. Both are minimum temperatures. Results are shown in Table 4.1.

It can be seen from the table that at short fill time the pressure is very high because of high flow rate required. As the filling slows down pressure drops. However, if the fill time is too long the plastic will get cold at the end of flow and viscosity will increase which will cause the pressure to rise again. Therefore, it is suggested not to mould the part slower than this fill time.

The limitation of maximum pressure depends upon the the machine capacity. A typical injection moulding machine can apply a pressure upto 100 MPa. So, the filling time which requires more than 100 MPa pressure should be neglected.

Now if the temperature at the end of flow becomes too small there will be problems at the end of flow such as bad finish, weld lines, etc. To achieve a reasonably uniform temperature distribution throughout the cavity, the temperature at the end of flow should not be more than 5 $°C$ higher than the temperature at entrance of the cavity and not less than $15°C$ lower than the temperature at the entrance of the cavity. The combination of mould tem-

Table 4.1: Mould temperature=$60^\circ C$, Melt temerature=$200^\circ C$ for LDPE

Filling time *Sec.*	Exit Temperature $^\circ C$	Max.Injection Pressure MPa	Remarks
.01	214.02	133.95	Not Feasible
.06	219 18	105.69	Not Feasible
.10	213.03	46.66	Not Feasible
.15	209.23	44.70	Not Feasible
.20	205 97	42.73	Not Feasible
.25	203.12	41.31	Feasible
.30	200 58	40.24	Feasible
35	198 26	39.41	Feasible
.40	196.10	38.73	Feasible
.45	194.08	38.16	Feasible
.50	192.16	37.68	Feasible
.55	190 33	37.25	Feasible
.60	188.57	32.82	Feasible
.65	186.88	36.55	Feasible
.70	185.26	36.27	Feasible
.75	183.69	36.14	Not Feasible
.85	181 09	38.71	Not Feasible
.90	180.08	55.42	Not Feasible
.95	177.71	31.21	Not Feasible
1.00	176.34	29.05	Not Feasible

perature,melt temperature and filling time which satisfies the above criteria is taken as feasible combination.

The results for other combination are shown in Table 4.2, Table 4.3, and Table 4.4. At the end of the process, eight boundary moulding conditions can be obtained as shown in Table 4.5.

Table 4.2: Mould temperature=60°C, Melt temerature=240°C for LDPE

Filling time *Sec.*	Exit Temperature °C	Max.Injection Pressure MPa	Remarks
.01	247.61	115.34	Not Feasible
.02	251.70	86.36	Not Feasible
.10	247.58	38.45	Not Feasible
.15	243.93	36.86	Feasible
.20	240.70	35.26	Feasible
.25	237.80	34.15	Feasible
.30	235.15	33.34	Feasible
.35	232.66	32.74	Feasible
.40	230.32	32.26	Feasible
.49	226.35	31.62	Feasible
.55	223.85	31.30	Feasible
.60	221.84	31.07	Not Feasible
.65	219.88	27.23	Not Feasible
.70	217.98	30.73	Not Feasible
.75	216.11	30.71	Not Feasible
.80	214.30	31.11	Not Feasible
.85	212.80	33.68	Not Feasible
.90	213.39	55.57	Not Feasible
.95	209.10	26.64	Not Feasible
1.00	207.43	26.55	Not Feasible

Table 4.3: Mould temperature=80°C. Melt temerature=200°C for LDPE

Filling time *Sec.*	Exit Temperature °C	Max.Injection Pressure MPa	Remarks
.01	219.13	119.38	Not Feasible
.06	220.07	95.51	Not Feasible
.10	213.64	43.29	Not Feasible
.15	209.85	41.51	Not Feasible
.20	206.70	39.65	Not Feasible
.25	203.99	38.26	Feasible
.30	201.61	37.19	Feasible
.35	199.44	36.33	Feasible
.40	197.45	35.62	Feasible
.45	195.60	35.01	Feasible
.50	193.85	34.49	Feasible
.60	190.60	29.97	Feasible
.65	189.09	33.22	Feasible
.70	187.63	32.90	Feasible
.75	186.24	32.69	Feasible
.80	184.93	32.79	Feasible
.85	183.88	34.07	Not Feasible
.90	183.17	42.28	Not Feasible
.95	180.91	28.10	Not Feasible
1.00	179.71	26.14	Not Feasible

CENTRAL LIBRARY
I. I. T., KANPUR
A 126251

Table 4.4: Mould temperature=80°C, Melt temerature=240°C for LDPE

Filling time *Sec.*	Exit Temperature °C	Max.Injection Pressure MPa	Remarks
.01	251.31	104.05	Not Feasible
.06	252.99	83.38	Not Feasible
.10	247.80	35.88	Not Feasible
.15	244.19	34.40	Feasible
.20	241.07	32.87	Feasible
.25	238.31	31.76	Feasible
.30	235.79	30.94	Feasible
.35	233.47	30.30	Feasible
.40	231.27	29.79	Feasible
.45	229.19	29.36	Feasible
.50	227.20	29.00	Feasible
.55	225.29	28.69	Feasible
.60	223.44	25.16	Not Feasible
.65	221.30	28.14	Not Feasible
.75	218.22	27.89	Not Feasible
.80	216.58	28.10	Not Feasible
.85	215.14	29.67	Not Feasible
.90	215.04	41.07	Not Feasible
.95	211.86	24.07	Not Feasible
1.00	210.36	22.36	Not Feasible

Table 4.5: Approximate Feasible Moulding Space for LDPE

Serial No.	Filling time *Sec.*	Melt Temperature °C	Mould Temperature °C
1	.25(min)	200.00	60.00
2	.70(max)	200.00	60.00
3	.15(min)	240.00	60.00
4	.55(max)	240.00	60.00
5	.25(min)	200.00	80.00
6	.80(max)	200.00	80.00
7	.15(min)	240.00	80.00
8	.55(max)	240.00	80.00

Optimization:

The optimized value of Process Parameters for LDPE is shown below,

$F(x) = 0.20$
Mould Temperature = 62.67 °C
Melt Temperature = 234.58 °C
Maximum Injection Pressure= 32.587 MPa
Filling Time = 0.22 Seconds
Cycle Time = 14.2927 Seconds

Here, weights of design variabels are $\omega_1 = 1$, $\omega_2 = .01$, $\omega_3 = .01$(Choi et al., 1994). The comparison of results after optimization and at the eight boundary points of AFMS is shown in Tables 4.6 to 4.13.

Table 4.6: Comparisons of Result at Serial No. 1 of AFMS shown in Table 4.5 and result after optimization for LDPE

	Before Optimization	After Optimization	Improvement (percentage)
$F(x)$	2.29	0.2	91.26
Temperature Difference	2.04	0.02	99.02
Maximum Inj. Pressure	38.52	32.58	15.41
Cycle Time	11.93	14.29	-19.780
Filling Time	0.25	0.22	12

Table 4.7: Comparisons of Result at Serial No.2 of AFMS shown in Table 4.5 and result after optimization for LDPE

	Before Optimization	After Optimization	Improvement (percentage)
$F(x)$	15.38	0.2	98.69
Temperature Difference	14.48	0.02	99.86
Maximum Inj. Pressure	55.42	32.58	41.20
Cycle Time	12.58	14.29	-13.59
Filling Time	0.9	0.22	75.56

Table 4.8: Comparisons of Result at Serial No.3 of AFMS shown in Table 4.5 and result after optimization for LDPE

	Before Optimization	After Optimization	Improvement (percentage)
$F(x)$	3.79	0.2	94.73
Temperature Difference	3.65	0.02	99.45
Maximum Inj. Pressure	36.85	32.58	11.58
Cycle Time	13.86	14.29	-3.12
Filling Time	0.15	0.22	-46.67

Table 4.9: Comparisons of Result at Serial No.4 of AFMS shown in Table 4.5 and result after optimization for LDPE

	Before Optimization	After Optimization	Improvement (percentage)
$F(x)$	15.46	0.2	98.70
Temperature Difference	14.91	0.02	99.86
Maximum Inj. Pressure	31.29	32.58	-4.12
Cycle Time	14.26	14.29	-0.23
Filling Time	0.55	0.22	60

Table 4.10: Comparisons of Result at Serial No.5 of AFMS shown in Table 4.5 and result after optimization for LDPE

	Before Optimization	After Optimization	Improvement (percentage)
$F(x)$	3.91	0.2	94.88
Temperature Difference	3.66	0.02	99.45
Maximum Inj. Pressure	38.26	32.58	14.82
Cycle Time	19.55	14.29	26.89
Filling Time	0.25	0.22	12

Table 4.11: Comparisons of Result at Serial No.6 of AFMS shown in Table 4.5 and result after optimization for LDPE

	Before Optimization	After Optimization	Improvement (percentage)
$F(x)$	14.94	0.2	98.66
Temperature Difference	14.14	0.02	99.86
Maximum Inj.Pressure	32.79	32.58	0.63
Cycle Time	20.1	14.29	28.89
Filling Time	0.8	0.22	72.5

Table 4.12: Comparisons of Result at Serial No.7 of AFMS shown in Table 4.5 and result after optimization for LDPE

	Before Optimization	After Optimization	Improvement (percentage)
$F(x)$	4.02	0.2	95.02
Temperature Difference	3.87	0.02	99.48
Maximum Inj. Pressure	34.39	32.58	5.26
Cycle Time	21.77	14.29	34.35
Filling Time	0.15	0.22	-46.66

Table 4.13: Comparisons of Result at Serial No.8 of AFMS shown in Table 4.5 and result after optimization for LDPE

	Before Optimization	After Optimization	Improvement (percentage)
$F(x)$	14.17	0.2	98.58
Temperature Difference	13.62	0.02	99.85
Maximum Inj. Pressure	28.69	32.587	-13.58
Cycle Time	22.17	14.29	35.53
Filling Time	0.55	0.22	60

Material selection:

Similarly, the AFMS for POLYPROPYLENE can be found out,the processing range of parameters are,

Mould Temperature range : $60°C - 90°C$

Melt Temperature range : $220°C - 280°C$

The AFMS for POLYPROPYLENE is shown in Table 4.14.

Table 4.14: Approximate Feasible Moulding Space for POLYPROPYLENE

Serial No.	Filling time $Sec.$	Melt Temperature $^{\circ}C$	Mould Temperature $^{\circ}C$
1	.10(min)	220.00	60.00
2	1.00(max)	220.00	60.00
3	.01(min)	280.00	60.00
4	.79(max)	280.00	60.00
5	.11(min)	220.00	90.00
6	1.23(max)	220.00	90.00
7	.01(min)	280.00	90.00
8	.83(max)	280.00	90.00

On the basis of AFMS of LDPE and POLYPROPYLENE we can decide the better of two, by using the method described in article.4.4.

IMI of LDPE,

$$IMI_{ldpe} = \int_{0.15}^{0.8} \int_{60}^{80} \int_{200}^{240} dT_{melt} dT_{mould}\, dt \qquad (4.9)$$

$$\Rightarrow IMI_{ldpe} = 520$$

IMI of POLYPROPYLENE,

$$IMI_{pp} = \int_{0.01}^{1.23} \int_{60}^{90} \int_{220}^{280} dT_{melt} dT_{mould}\, dt \qquad (4.10)$$

$$\Rightarrow IMI_{pp} = 2196$$

Since, the IMI of POLYPROPYLENE is more than the LDPE, POLYPROPYLENE is better material for moulding the geometry described in the problem. Practically, it is also found that Polypropylene is better material than LDPE for injection moulding purpose, this fact validates the IMI.

It may be noted material selection is based only on two variables for the sake of demonstration of the method. However, cost of material is not used as one of the criteria for optimization.

Chapter 5

CONCLUSIONS AND SCOPE FOR FUTURE WORK

In the present work, numerical simulation of the mould-filling for the production of a cylindrical object using LDPE as the material is presented first. Finite-difference method is used for the purpose of modelling. Three cases have been considered, namely (*i*) Isothermal filling at constant injection pressure,(*ii*) Isothermal filling at constant flow rate and (*iii*) Non-isothermal filling at constant flow rate. The results show excellent tally with the corresponding analytical solutions for the first two cases showing the correctness of the numerical method. The simulation results for non-isothermal filling show physically realistic trends and lend insight into various important aspects of mould-filling including frozen skin layer. The final part of the thesis deals with optimization of moulding conditions for the same object and material selection. The exhaustive search method is used for optimization. The cooling of the object is also considered. It is found that between LDPE and Polypropylene, the latter is a better material for the production of this object.

5.1 Scope For Future Work

Future work can be done along the following lines. First, experimental validation of the numerical results for the non-isothermal filling can be performed. Secondly, the material and manufacturing cost and larger material data base can be included in the optimization procedure for more realistic study. Finally, numerical simulation of cooling can be done to make the injection moulding study a complete one. The study can also be extended to more complicated geometry.

Bibliography

[1] Bernhardt, Ernest C., 1962, *Processing of the Thermoplastic Materials*, Reinhold Publishing corporation. New York., pp. 308-372.

[2] Bown, John, 1979, *Injection Molding of Plastic Components*. McGraw-Hill, U.K., pp. 88-146.

[3] Chen, B.S.,and Liu, W.H., 1994, "Numerical simulation of the post filling stage in Injection Molding with a Two-Phase Model", *Polymer Engineering and Science*, Vol.34, No.10, pp. 835-846

[4] Chiang, H.H., Hieber, C.A., and Wang, K.K., 1991, "A Unified Simulation of the Filling and Post filling stages in Injection Molding PartI: formulation", *Polymer Engineering and Science*, Vol.31, No.2, pp. 116-123.

[5] Choi, G.H., Lee, K.D., and Chang, N., 1994, "Optimization of Process Parameters of Injection Molding with Neural Network App.lication in a Process Simulation Environment" *Annals of the CIRP*, Vol.43. No.1, pp. 449-452.

[6] Guceri, Selcuk I., 1989, "Finite Difference Solution of Field Problems"(*Computer Modeling for Polymer Processing, Ed. Charles L. Tucker III*), Hanser Publishers, pp. 142-236

[7] Holman, J.P., 1997, *Heat Transfer*, McGraw-Hill, Inc. 8th Ed.

[8] Hieber, C.A., and Shen. S.F., 1980, "A Finite-Element/Finite Difference Simulation of the Injection Molding Filling Process", *J. non-Newtonian Fluid Mechanics*, Vol.7, pp 1-32.

[9] Hetu, J.F., Gao, D.M., Garcia-Rejon, A., and Salloum, G., 1998, "3D Finite Element Method for the Simulation of the Filling Stage in Injection Molding", *Polymer Engineering and Science*, Vol.38, No.2, pp. 223-236.

[10] Jaluria, Yogesh, 1988, *Computer Methods for Engineering*, Allyn and Bacon, Inc.

[11] Kamal, M.R., Mashelkar, R.A., and Mujumdar, A.S., 1989, *Transport Phenomenon in Polymer Systems -2*, Willey Eastern Ltd., pp. 133-217

[12] Kamal, M.R., and Kenig, S., 1972, "The Injection Molding of Thermoplastics" , *Polymer Engineering and Science*, Vol.12, pp. 294-302.

[13] Kamal, M.R., Mutel, A.T., Garcia-Rejon, A., and Salloum, G., 1991, *SPE ANTEC Tech Papers*, Vol37, pp. 483

[14] Pandelidis, Ioannis., and Zou, Qin., 1990, "Optimization of Injection Molding Design. PartI: Gate Location Optimization", *Polymer Engineering and Science*, Vol.30, No.10, pp. 873-882.

[15] Pandelidis, Ioannis., and Zou, Qin., 1990, "Optimization of Injection Molding Design. PartII: Molding Condition Optimization", *Polymer Engineering and Science*, Vol.30, No.10, pp. 882-892.

[16] Wu, P.C., Huang, C.F., and Gogos, C.G., 1974, "Simulation of the Mold-Filling Process", *Polymer Engineering and Science*, Vol.14, No.14, pp. 223-230.

[17] Tadmor, Zehev and Gogos, Costas.G., 1979, *Principles of Polymer Processing*, John Willey and Sons.

Appendix A

CALCULATION OF INJECTION PRESSURE FOR CASE II AND CASE III BY NEWTON-RAPHSON METHOD

According to Newton-Raphson method, the roots of an algebraic equation can be found by repeatedly using the Eq.(A.1).

Let $f(x) = 0$ be the equation for which roots are to be found out . It can be proved (Jaluria,1988) that

$$x_{i+1} = x_i - \frac{f(x_i)}{f'(x_i)} \qquad (A.1)$$

where x_{i+1} is the improved root while x_i is the guessed root.

The iteration stops when $| x_{i+1} - x_i | \leq \epsilon$ where ϵ is a very small value like 0.01, 0.001 etc.

The above concept can be used to solve for the injection pressure at various times for isothermal as well as non-isothermal constant flow rate filling problems.

If Q is the flow rate, then for the correct P_{inj}, we can write

$$F(P_{inj}) = \int_0^R V_z 2\pi r dr - Q = 0 \qquad (A.2)$$

That is, P_{inj} is the root of the Eq.(A.2).

Now, following Newton-Raphson procedure as described by Eq.(A.1), we can write

$$P_{inj,improved} = P_{inj,guess} - \frac{F(P_{inj})_{guess}}{F(P_{inj})_{guess1} - F(P_{inj})_{guess2})/\Delta P_{inj}} \qquad (A.3)$$

ΔP_{inj} is taken as a small interval

The procedure is repeated till

$$\mid P_{inj,improved} - P_{inj,guess} \mid \leq \epsilon \; .$$

Appendix B

CALCULATION OF COOLING TIME FROM THE EQUATION OF BERNHARDT(1962)

Bernhardt(1962) gave an account of an experiment work in determining moulding 'set-up' time(that is, the time for a moulding, in the mould, to become hard enough to remove) and put forward an equation by which it could be calculated.

$$t_c = -\frac{(0.0004S)^2}{2\ \pi\ \alpha^2}[\log\ \theta - log\ 0.81] \qquad (B.1)$$

where,

$$\theta = \frac{T_\alpha - T_{mould}}{T_{melt} - T_{mould}}$$

t_c is the set-up or cooling time in seconds
S is the surface area of the cavity in (cm^2)
α is the thermal diffusivity in (cm^2/sec)
T_x is the heat distortion temperature$(°C)$
T_{melt} is Melt temperature$(°C)$
T_{mould} is Mould temperature$(°C)$

Eq(B.1) has been found to give good results for polysterene but can also be used to a resonable approximation for other thermoplastics such as LDPE, Polpropylene, etc.

The input data used for the optimization study for LDPE and Polypropylene are shown in Table B.1 and Table B.2 respectively.

Table 5.1: Input Data for LDPE(Bown,1979)

Thermal diffusivity	0.0027 (cm^2/s)
Heat distortion temperature	90 $^\circ C$

Table 5.2: Input Data for Polypropylene(Bown,1979)

Thermal diffusivity	0.0013(cm^2/s)
Heat distortion temperature	120 $^\circ C$

A126251

Date Slip A126251

This book is to be returned on the date last stamped.

ME-1998-M-AMI-NUM

[redacted]

A126251